Posted on 17 Jan 2023 — The copyright holder is the author/funder. All rights reserved. No reuse without permission. — https://doi.org/10.22541/essoar.167397443.39838795/v1 — This a preprint and has not been peer reviewed. Data may be preliminary.

The impact of human-induced climate change on potential tornado intensity as revealed through multi-scale modeling

Matthew Woods[1], Robert Trapp[1], and Holly M. Mallinson[2]

[1]UIUC
[2]University of Illinois Urbana-Champaign

January 17, 2023

Abstract

A novel, multi-scale climate modeling approach is used to provide evidence of potential increases in tornado intensity due to anthropogenic climate change. Historical warm- and cool-season (WARM and COOL) tornado events are virtually placed in a globally warmed future via the "pseudo-global warming" method. As hypothesized based on meteorological arguments, the tornadic-storm and associated vortex of the COOL event experiences consistent and robust increases in intensity, size, and duration in an ensemble of imposed climate-change experiments. The tornadic-storm and associated vortex of the WARM event experiences increases in intensity in some of the experiments, but the response is neither consistent nor robust, and is overall weaker than in the COOL event. An examination of environmental parameters provides further support of the disproportionately stronger response in the cool-season event. These results have implications on future tornadoes forming outside of climatologically favored seasons.

The impact of human-induced climate change on potential tornado intensity as revealed through multi-scale modeling

Matthew J. Woods[1]†, Robert J. Trapp[2], and Holly M. Mallinson[3]

[1]Department of Atmospheric Sciences, University of Illinois.

[2]Department of Atmospheric Sciences, University of Illinois.

[3]Department of Atmospheric Sciences, University of Illinois.

Corresponding author: Robert J. Trapp (jtrapp@illinois.edu)

†Current affiliation: National Weather Service, Las Vegas, NV.

Key Points:

- The effects of climate change on tornado intensity have been unclear.
- A novel, multi-modeling approach is used to address such effects.
- The intensity of cool-season tornadoes would appear to be most susceptible.

Abstract

A novel, multi-scale climate modeling approach is used to provide evidence of potential increases in tornado intensity due to anthropogenic climate change. Historical warm- and cool-season (WARM and COOL) tornado events are virtually placed in a globally warmed future via the "pseudo-global warming" method. As hypothesized based on meteorological arguments, the tornadic-storm and associated vortex of the COOL event experiences consistent and robust increases in intensity, size, and duration in an ensemble of imposed climate-change experiments. The tornadic-storm and associated vortex of the WARM event experiences increases in intensity in some of the experiments, but the response is neither consistent nor robust, and is overall weaker than in the COOL event. An examination of environmental parameters provides further support of the disproportionately stronger response in the cool-season event. These results have implications on future tornadoes forming outside of climatologically favored seasons.

1 Introduction

Hazardous convective weather (HCW) in the form of damaging winds, hail, and tornadoes poses a serious threat to life and property in the United States. From 2012 to 2022, 95 HCW events produced over $1 billion (inflation-adjusted) in damages (NOAA, 2022). The frequency of these events has increased markedly since the start of the 21st century, owing in part to increased exposure and population density (Strader et al., 2017), but also potentially to anthropogenic climate change (ACC).

HCW depends on the 3D characteristics of environmental temperature, humidity, and wind, which are projected to change under ACC. For example, warming and humidification of lower-tropospheric air yields increases in convective available potential energy (CAPE), which leads to increases in the potential intensity of convective-storm updrafts. Conversely, relatively more warming at high latitudes weakens the meridional temperature gradient and thus the vertical shear of the horizontal wind (hereinafter, VWS); this suggests a reduction in the tendency for convective updrafts to develop significant, long-lived rotational cores. General circulation model (GCM) and regional climate model (RCM) simulations project decreases in VWS that are disproportionately smaller than increases in CAPE, indicating an increase in frequency and/or

intensity of future HCW events under ACC in the United States (e.g., Del Genio et al., 2007; Trapp et al., 2007; Trapp et al., 2009; Gensini et al., 2014; Diffenbaugh et al., 2013; Seeley & Romps, 2015; Hoogewind et al., 2017). Of relevance herein is the seasonal non-uniformity to this increase: Boreal winter tends to exhibit the largest relative increase in the CAPE–VWS covariate (Diffenbaugh et al., 2013). This is consistent with historical trends of environmental parameters computed using reanalysis data (Gensini & Brooks, 2018).

Precisely how these conclusions relate to *tornado intensity*, and thus address the very basic question of whether tornadoes will tend to be more intense under ACC, is unclear. Although trends in increasingly powerful tornadoes have been revealed in historical tornado damage data in the U.S. (Elsner et al., 2019), these have not yet been physically linked to ACC. This is partly because relationships between observed tornado intensity and environmental parameters such as CAPE and VWS are ambiguous. For example, although nonzero CAPE is considered a necessary condition for, and thus critically relevant to tornadic-storm formation, CAPE alone does not correlate well with observed tornado intensity (Thompson et al., 2012). As supported by our analyses in section 3.3, a possible link could be made using multivariate environmental parameters such as the significant tornado parameter (STP), which appears to better discriminate environments of significant tornadoes from those of nonsignificant tornadoes (Thompson et al., 2012), although still not perfectly. However, an environment-only argument has a critical limitation, namely, that realization of a significant tornado is conditional on tornadic-storm initiation, which STP does not unambiguously predict. Indeed, the mean frequency of storms that initiate given a supportive environment is non-uniform in time and space, and even appears to change under ACC (Hoogewind et al., 2017).

Explicit climate modeling of tornadoes is an alternative to the use of environmental parameters and removes the storm-initiation limitation. Although such an approach has been computationally prohibitive because of the small-scale of tornadoes (~100 m to 1 km), multi-scale modeling now offers a tractable solution. Herein we employ the pseudo global warming (PGW) methodology (Schär et al., 1996; Frei et al., 1998; Kimura & Kitoh, 2007; Sato et al., 2007) using a novel, multi-scale, multi-model approach. Briefly, PGW involves a comparison of simulations of events under their true 4D environment (the control; CTRL) with those under a 4D environment modified by a climate-change perturbation representative of *mean atmospheric conditions* over future and historical time slices. Thus, the PGW method allows for an isolation of the response of an event to an imposed ACC. Because *event-level* PGW applications (see Trapp et al., 2021) involve relatively short time integrations, they also allow for the use of higher resolution and multiple realizations.

Two archetypal yet regionally and seasonally contrasting events are considered. The first is the 10 February 2013 (hereinafter, COOL) event that includes the EF-4 tornado in Hattiesburg, Mississippi, and the second is the 20 May 2013 (hereinafter, WARM) event that includes the EF-5 tornado in Moore, Oklahoma. Together, these tornadoes were responsible for 24 fatalities, more than 300 injuries, and approximately $2 billion in damage (NOAA, 2013). Our working hypothesis is that the WARM event will exhibit relatively less intensity changes under PGW than the COOL event.

Analyses of these event simulations provide the initial means to address this hypothesis. However, the spatio-temporal representations of the tornadic storms, and even the total numbers of storms, are different between the PGW and CTRL simulations (see Fig. 1). This implied lack of a clear CTRL–to–PGW comparison of *specific* tornadic storms means that a quantitative

evaluation of the climate change effect on the intensity of *specific* tornadoes is tenuous. Accordingly, we introduce an additional step wherein an idealized numerical model is integrated using initial and boundary conditions (ic/bc) drawn from the regional-model simulations. The relatively reduced complexity and higher spatial resolutions afforded by this idealized-modeling implementation of the PGW methodology helps further isolate the climate change response on a single storm, and allows for explicit diagnoses of tornado intensity.

2 Materials and Methods

2.1 PGW approach

The PGW climate modeling approach involves a simulation of some event under its actual, present-day forcing, and then simulations of the event under a modification of this forcing. The modification comes from the addition of a climate-change delta, which herein is the difference between mean conditions over future and historical time slices during a relevant month. Separate sets of deltas are constructed using historical and Representative Concentration Pathway 8.5 simulations from each of five GCMs (GFDL-CM3, MIROC5, NCAR-CCSM4, IPSL-CM5A-LR, and NorESM-1M). The GCM data originate from the Coupled Model Intercomparison Project phase 5 (Taylor et al., 2012), and provide a range of convective-storm environments over historical and future time periods (Diffenbaugh et al., 2013; Seeley & Romps, 2015).

Three different formulations of the climate-change deltas (see Trapp et al. 2021), computed using five different GCMs, provide an ensemble of 15 simulations plus an additional composite-delta simulation to assess the PGW response of each event. Because these 16 different deltas explicitly represent a range in the climate-change signal, we argue that their use toward generation of an ensemble is more relevant than other approaches. Specifically, and importantly, we are

interested in the model response to the imposed climate change and associated ic/bc rather than in the model response to variations in parameterization schemes, etc.

2.2 Regional model configuration

The CTRL and PGW simulations of the WARM and COOL events are performed using version 4.0 of the Weather Research and Forecasting model (WRF) (Skamarock et al., 2008). The parent computational domains have horizontal grid spacings of 3 km. Subdomains of 1-km grid spacing are nested within the parent domains over central Oklahoma and central Mississippi, respectively (Fig. S1). The results reported in section 3.1 are based on analyses over the nested domains.

The simulations are initialized at 12 UTC for both events. This allows for more than six hours of "spin-up" time prior to the observed EF-5 Moore and EF-4 Hattiesburg tornadoes, which is typical for weather-event simulations with WRF (Skamarock, 2004). Initial and boundary conditions are derived from the North American Mesoscale Forecast System analysis. Additional details regarding WRF model configuration can be found in Trapp et al. (2021). Decisions on the configuration and on the ultimate veracity of the CTRL simulations were established by comparing model output from configuration-sensitivity experiments to observed radar characteristics and tornado reports, as described in Woods (2021).

Upon adapting the approach of Sherburn & Parker (2019), local tornado occurrence and potential intensity are diagnosed using the Okubo-Weiss (OW) parameter. OW is computed at 80 m AGL as the difference between vertical vorticity squared and deformation squared (e.g., Markowski et al., 2011); the choice of 80 m is based on its use in operational applications. At the 1-km gridpoint spacings of the WRF simulations, tornadoes are still unresolved, so OW is used

as a proxy: An OW value locally exceeding 3.5×10^{-5} s^{-2}, which is the 90th percentile of all gridpoint values with positive OW in the CTRL simulation, serves as a tornado proxy occurrence. An OW value exceeding 6×10^{-5} s^{-2}, which is the 95th percentile, serves as a significant tornado proxy occurrence. Coexistence of local updraft velocities exceeding 5 m s^{-1} is also required. Differentiating tornado intensity based on OW and thus tornadic-circulation strength follows from Doppler radar-based studies of Toth et al. (2012) and others. Owing in part to the discreteness of the OW calculations, there is no expectation of a one-to-one correspondence between the numbers of tornadoes and tornado proxies. Rather, the proxy occurrences should be viewed in a relative sense, which is how the results are presented in section 3.1.

2.3 Idealized model configuration

The idealized simulations are performed using Cloud Model 1 (CM1) (Bryan & Fritsch, 2002). Grid stretching is employed such that the horizontal grid spacing is 64 m over the inner 80 x 80 km of the 180 x 180 x 18.5 km model domain, and then increased to 2.5 km at the domain edges. Vertical grid spacing is stretched from 20 m in the lowest 300 m to 250 m in the upper 6000 m, with 125 m grid spacing in between. Additional details regarding the CM1 model configuration can be found in Woods (2021). Note that the actual tornadoes that occurred on 20 May 2013 and 10 February 2013 had damage widths of 1600 m and 1200 m, respectively. Even if the core diameters of maximum winds of these tornadoes were 50% of these widths, the cores would still be represented by ~10 grid points. So, although our simulations do not have grid spacings appropriate to resolve fine-scale structures of the tornadoes, the simulations are

certainly sufficient to represent core widths and windspeeds, which is one goal of these simulations.

The initial and boundary conditions are drawn from the WRF output of the CTRL and PGW simulations. Specifically, 60 x 60 km horizontal averages centered about the WRF grid point nearest to Moore, Oklahoma and Hattiesburg, Mississippi are used to obtain vertical profiles at 20 UTC 20 May 2013 and 23 UTC 10 February, respectively, which represent well the pre-tornadic conditions during these two events. A single deep convective storm is initiated within these environments via updraft nudging (Naylor & Gilmore, 2012) that persisted for 20 minutes. Our analysis of the subsequent tornadic circulations began at 30 min, i.e., 10 min after the cessation of the nudging.

Tornadic-like vortices (TLVs) are identified by examining near-surface fields of windspeed, vertical vorticity, and OW parameter. Following Sherburn & Parker (2019), TLV identification required vertical vorticity, windspeed, and OW to exceed 0.1 s^{-1}, 30 m s^{-1}, and 0.03 s^{-2}, respectively, and be collocated with low-level updraft speeds exceeding 5 m s^{-1}. Upon locating the strongest TLV, maximum and minimum of *x*-direction and *y*-direction wind components are found within 500 m of the vortex center. The locations of these maxima and minima are used to determine an average radius (r) of maximum winds (V).

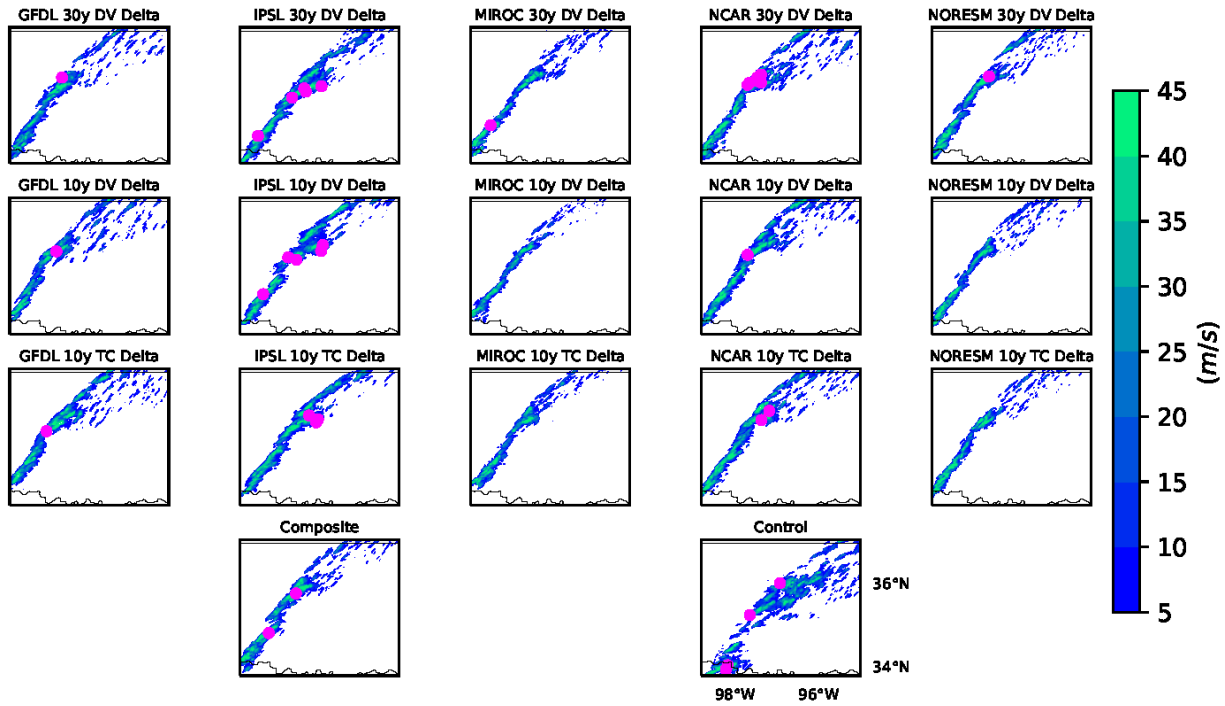

177

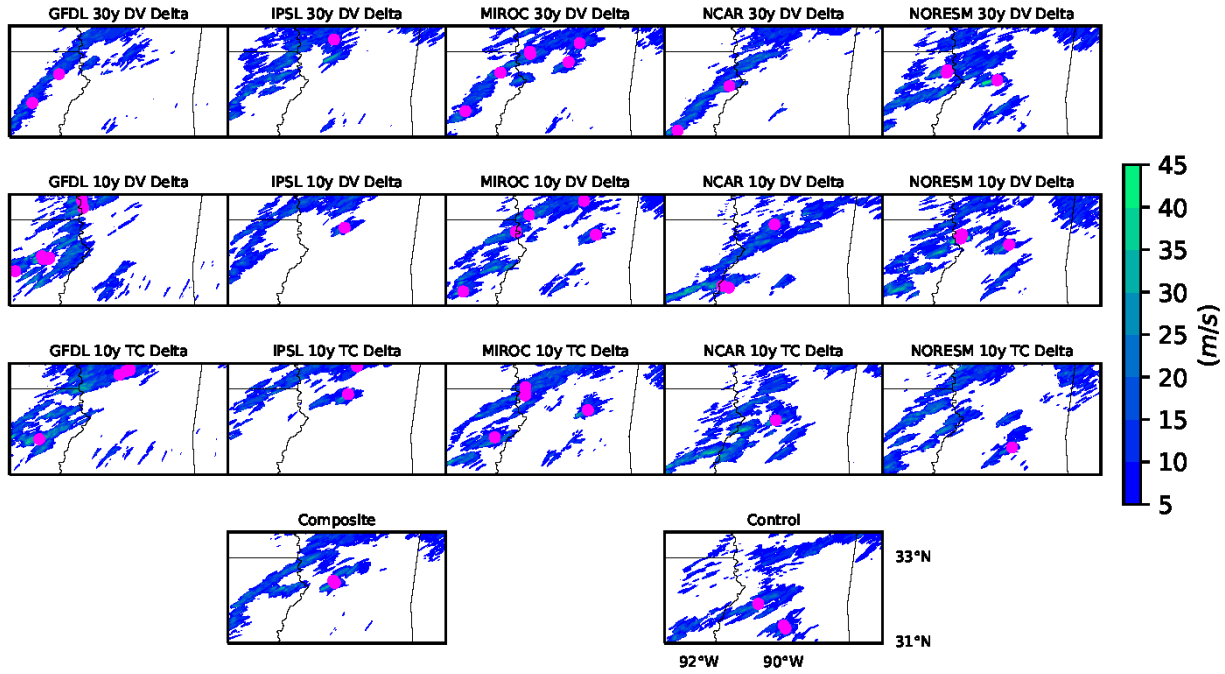

178

179 **Figure 1.** Locations of model-diagnosed tornadic circulations (magenta dots) and column-
180 maximum updraft speeds (m s^{-1}) for the regional-modeling simulations of the WARM event at
181 2100 UTC (upper panels), and COOL event at 2230 UTC (lower panels). In addition to the
182 CTRL simulation, the subpanels indicate an individual experiment composing the ensemble.
183

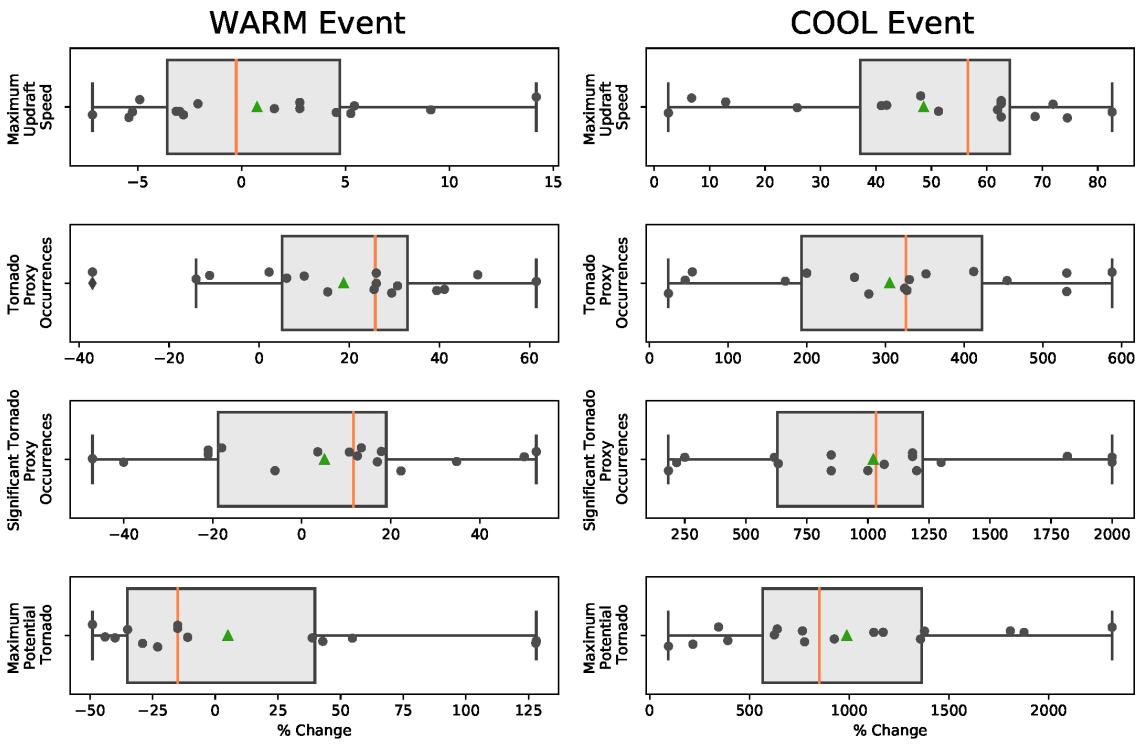

Figure 2. Box-and-whisker plots of tornadic-storm intensity metrics, as evaluated from the regional modeling simulations of the WARM event (left) and COOL event (right). Values of these metrics are given as percentage changes in the PGW simulations relative to the control (CTRL) simulation. The median is the orange line, mean is the green triangle, and individual data points are the black circles.

3 Results

3.1 Regional-modeling perspective

An ensemble of 16 simulations is used to assess the PGW response of each event. The ensemble members are meant to represent a range of possible future realizations of the event. Herein, if 75% of the ensemble members exhibit the same sign in the percentage change (PGW relative to CTRL) in a given metric, we consider the PGW response for that metric to be *consistent*. If we equate the signal in the metric to the mean value across the ensemble, and the

noise to the standard deviation, the response in this metric is considered to be *robust* (*highly robust*) if the PGW signal-to-noise ratio in a given metric exceeds one (two) (e.g., Diffenbaugh et al., 2013).

We begin with two metrics that provide information on overall storm intensity. The first is the cumulative gridpoint exceedance of 55 dBZ simulated radar reflectivity (Fig. S2). This metric quantifies the total area of intense convective storms over a given simulation. A consistent, robust response is shown in this metric, as represented by an average percentage increase of +110% (PGW exceedances relative to those in the CTRL) (Fig. 2a). Thus, the PGW-modified conditions resulted in relatively more extensive and intense convective storms in association with the WARM event.

Cumulative gridpoint exceedances of simulated updraft speed confirm this increase in the extent of intense convective storms under PGW (Fig. S3); this consistent, robust response is represented by an average percentage increase of +40%. The *peak* updraft speeds are comparatively stronger in only half of the PGW simulations, with an average percentage increase of +1% (Fig. 2). These results indicate that intense convective updrafts in a future realization of the WARM event would be more numerous or larger, but not always stronger.

In terms of the occurrences of our tornado proxy, the PGW response is inconsistent albeit robust, with a mean percentage *decrease* of -7% (Fig. 2). For occurrences of our significant tornado proxy, the mean response is inconsistent but highly robust, with a mean percentage decrease of -19% (Fig. 2). Finally, when we evaluate the peak OW per PGW simulation, which provides some information about the potential tornado intensity, we find this response to be consistently negative but not robust, with an average percentage difference (PGW values relative

to those in the CTRL) of -11% (Fig. 2). Thus, the regional modeling suggests relatively fewer and weaker tornadoes in the WARM event under PGW, albeit with uncertainty (see also Fig. 1).

Like the WARM event, the COOL event under PGW also tends to be characterized by more intense convective storms. Specifically, cumulative gridpoint exceedances of simulated reflectivity of 55 dBZ are greater in all but one of the PGW simulations, thus contributing to an average percentage increase of +125%, and a consistent and robust response in this metric (Fig. S2). The other metric for overall storm intensity, cumulative gridpoint exceedances of updraft speed of 25 m s^{-1}, is consistent but not robust; notably, the average percentage increase in such strong updraft occurrence in the COOL event is +712%, as compared to the +40% increase associated with the WARM event (see Fig. S3). *All* PGW simulations had peak updraft speeds exceeding the 31 m s^{-1} peak of the CTRL (Fig. 2), thus implying a consistent and robust response. Moreover, half of the PGW simulations had peak updrafts exceeding 50 m s^{-1}, which historically are speeds more readily supportive in warm-season, Great Plains environments than in cool-season, southeast U.S. environments. These results indicate that intense convective updrafts in a future realization of the COOL event would be more numerous *and* stronger.

Occurrences of the tornado proxy are substantially greater under PGW in many of the simulations, leading to an average percentage increase relative to CTRL of +163% (Fig. 2). Occurrences of the significant tornado proxy are also substantially greater, with an average percentage increase of +642%, in this consistent and robust response (Fig. 2). Finally, a consistent and robust response is indicated in the peak OW per PGW simulation, and thus potential tornado intensity, with an average percentage increase of +756% (Fig. 2).

Collectively, these results suggest that tornadic circulations in a future realization of the COOL event would be more numerous, stronger, and perhaps longer-lived. In agreement with

our hypothesis, the magnitude of the response of this archetypal cool-season event to PGW is much larger than that of the archetypal warm-season event; this finding is also in agreement with Bercos-Hickey et al. (2021). There is still, however, ambiguity in precisely how the analyzed response relates to tornado intensity, given both the model grid resolution and the nature of the tornado proxy. Thus, we now use the TLV–resolving idealized PGW simulations to compute explicit measures of tornado intensity, and thus help clarify the regional-model results.

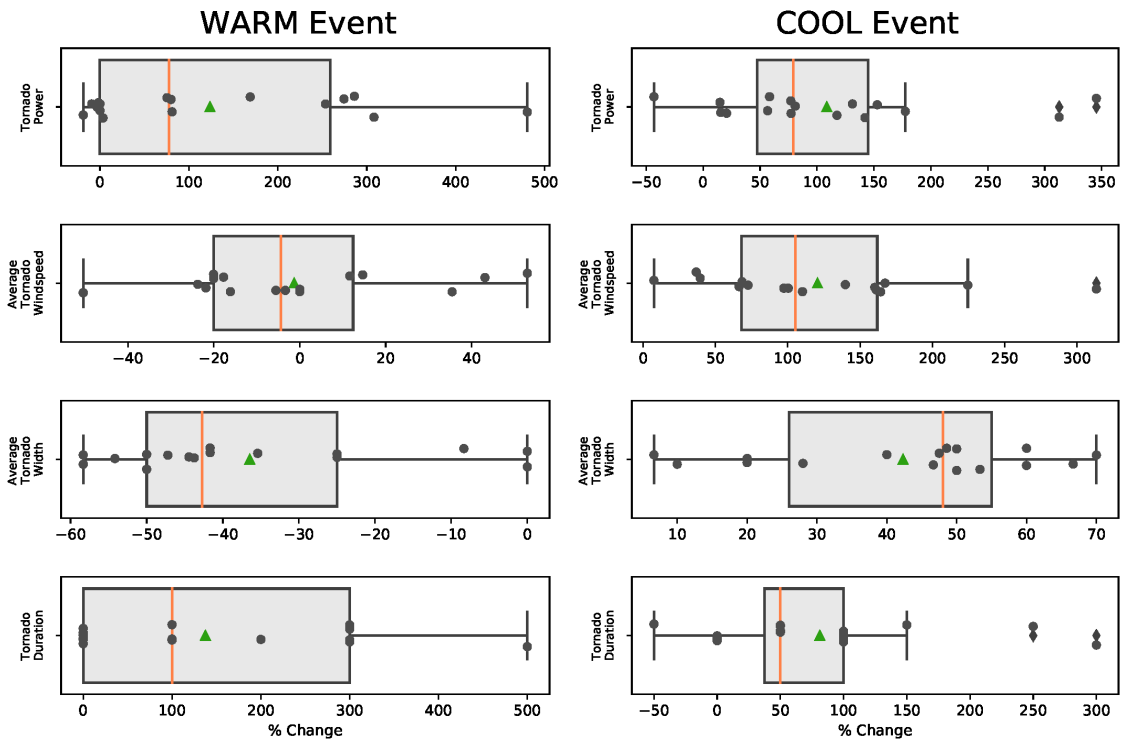

Figure 3. As in Figure 2, except for tornado intensity metrics (see text).

3.2 Idealized modeling perspective

The idealized PGW simulations have steady, horizontally homogeneous initial and boundary conditions that were drawn from the regional-model simulations of the WARM and COOL events (Figs. S4-S5). The much finer grid spacings (64 m) allow for explicit

quantifications of TLVs that form within the simulated storms. For this we use *tornado power*, which accounts for the tornadic wind speed as well as the width and length of the tornado track. As adapted from Fricker et al. (2014), instantaneous tornado power can be calculated as

$$P = \pi r^2 \rho V^3 \qquad (1)$$

where r represents the average radius of maximum winds, ρ is the air density (assumed to be 1 kg m^{-3}), and V is the average maximum surface wind speed at radius r. Total tornado power here is the summation of $\log(P)$ over the lifetime of the tornado-like vortex,

$$P_t = \sum \log(P) \qquad (2)$$

In simulations of the WARM event, the PGW response in total power is neither consistent nor robust. However, the 16-member ensemble contributed to an average percentage increase in P_t of +124% (Fig. 3). This average percentage increase is due to a few experiments with relatively stronger vortex windspeeds; none of the experiments exhibited wider vortices (Fig. 3). Thus, as in the coarser-resolution regional modeling simulations, there are indications of intensity increases in this violent, Great Plains, warm-season tornado given an imposed climate change.

For the COOL event, the PGW response in total power is both consistent and robust, with an average percentage increase of +109% (Fig. 3). The increases in P_t are driven by consistent and robust increases in tornadic-vortex strength and width (Fig. 3). The relatively longer duration of the tornadic vortices (+81%) also contribute to the larger P_t under PGW. These high-resolution simulations are in agreement with the regional modeling simulations, and clearly demonstrate an increased intensity and duration for this archetypal cool-season tornado given an imposed climate change. The collective simulations also confirm our hypothesis regarding a relatively larger response of this cool-season event.

Table 1. Mean values, and percentage changes relative to the CTRL experiment, of environmental parameters computed from the initial/boundary conditions of the idealized-modeling PGW experiments.

Event	CAPE (J/kg)		CIN (J/kg)		LCL (m)		SRH3 (m2/s2)		SRH1 (m2/s2)		S06 (m/s)		STP	
WARM	4484	+56	0	+100	1774	+23	86	-58	34	-53	24	-14	0.2	-72
COOL	1037	+162	-24	-61	243	+33	427	-21	327	-23	36	-4	2.2	+100

CIN is convective inhibition; LCL is lifting condensation level; SRH3 is storm-relative environmental helicity, evaluated over the 0-3 km layer; SRH1 is storm-relative environmental helicity, evaluated over the 0-1 km layer; S06 is the bulk wind shear, evaluated over the 0-6 km layer.

We can use the ic/bc of the idealized experiments to explore the meteorological arguments on which this hypothesis is based. The mean, PGW-enhanced CAPE of 4484 J kg^{-1} and 1037 J kg^{-1} for the WARM and COOL events, respectively, represent consistent and robust increases of +56% and +162% relative to the corresponding CTRL environments (Table 1). The mean, PGW-diminished VWS of 24 m s^{-1} and 36 m s^{-1} for the WARM and COOL events, respectively, represent consistent and robust decreases of -14% and -4% relative to the corresponding CTRL environments (Table 1); disproportionate decreases of storm-relative helicity, another measure of VWS, are also revealed for the WARM versus COOL events (-53% and -23%, respectively; Table 1). When these and other environmental parameters are combined through the multivariate parameter STP, the environment of the WARM event is found to be relatively *less* supportive of a significant tornado under PGW (mean percentage decrease of -73%), while the environment of the COOL event is relatively *more* supportive under PGW (mean percentage increase of +100%) (Table 1).

3.3 Generality of the conclusions

306 Although the intensity changes described herein apply to the specific WARM and COOL
307 events simulated, all potential tornadic-storm events realized during the warm- and cool-season
308 months of consideration would be subject to the same range of climate-change perturbations. To
309 help quantify how these perturbations alone might contribute to environments of significant
310 tornadoes, STP is calculated at all points within the regional-model domain for the CTRL and
311 PGW simulations of both events (Fig. S7). Upon spatially averaging the PGW – CTRL
312 differences, we find that the ensemble mean STP perturbation is -0.30 for the month of May, and
313 +0.70 for the month of February. The implication is that ACC would contribute, *on average*, to
314 environments that are relatively *less* supportive of a significant tornado during May across the
315 central Great Plains U.S., and relatively *more* supportive of a significant tornado during February
316 across the southeast U.S. Such environmental changes have been noted in studies by Gensini &
317 Brooks (2018), Bercos-Hickey et al. (2021), and Lepore et al. (2021).

318

319 **4 Summary and Conclusions**

320 Although trends in increasingly powerful tornadoes have been suggested in historical
321 data on tornado damage (Elsner et al., 2019), our study is the first to provide evidence of
322 potential increases in future tornado intensity due to ACC.

323 This statement applies explicitly to two contemporary, archetypal, warm- and cool-season
324 tornado events that were virtually placed in a globally warmed future via the PGW method.
325 Specifically, the consistent and robust increases in intensity, size, and duration of the tornadic-
326 storm and associated vortex of the COOL event can be attributed directly to ACC. The lack of a
327 consistent and robust increase in the intensity of the tornadic-storm and associated vortex of the

WARM event can likewise be attributed directly to ACC. Consideration of other data lends support to such a disproportionate response based on season of the year.

The preceding statement should not be interpreted to mean that *all* tornadoes will be stronger in the future. The atmospheric heterogeneity arising from naturally variable large-scale atmospheric circulations, high-frequency weather systems, convective storms and their residual effects, and land-surface variations (e.g., see Trapp, 2013) will continue to create diverse environmental conditions both supportive and non-supportive of thunderstorm formation. Significant tornadogenesis within such thunderstorms will also continue to require a delicate balance between VWS and CAPE, among other environmental parameters. Yet because cool-season environments in the current climate tend to be characterized by very large VWS and small CAPE, future increases in CAPE (decreases in VWS) due to ACC appear to be relatively more conductive to (less impactful on) this balance and thus on cool-season tornado potential.

These findings have implications on the possible impacts of future tornadoes forming outside of climatologically favored seasons, in the United States and elsewhere around the world. Indeed, situational awareness of tornado risk tends to be reduced during seasons such as boreal winter, which offers one explanation for high fatalities from tornadic events during these times (e.g., Ashley, 2007). It follows that more intense future tornadoes would have the potential to result in more fatalities and damage.

Acknowledgments

This research was supported by the National Science Foundation, award AGS 1923042. The WRF simulations were conducted on the NCAR Cheyenne Computing Facility. The CM1 simulations were conducted on the Blue Waters Petascale Computing Facility. We thank Dr.

George Bryan for making available and otherwise supporting the CM1 model. We acknowledge the World Climate Research Programme's Working Group on Coupled Modelling, which is responsible for CMIP, and we thank the climate modeling groups indicated in section 2.1 for producing and making available their model output.

Open Research

The following GCM data sets used in this study are available through the CMIP5 repository (https://esgf-node.llnl.gov/projects/cmip5/), using these criteria: Models: GFDL-CM3, MIROC5, NCAR-CCSM4, IPSL-CM5A-LR, and NorESM-1M; Experiments: historical and RCP8.5; Ensemble: r1i1p1; Realm: atmos; and Time Frequency: 3hr or 6hr. The WRF model is available at https://www2.mmm.ucar.edu/wrf/users/, and the CM1 model is available at https://www2.mmm.ucar.edu/people/bryan/cm1/. Relevant simulation data are available through the Illinois Data Bank at https://databank.illinois.edu/datasets/IDB-4479773#.

References

Ashley, W. S. (2007). Spatial and Temporal Analysis of Tornado Fatalities in the United States: 1880–2005. *Weather and Forecasting*, *22*(6), 1214–1228. https://doi.org/10.1175/2007WAF2007004.1

Bercos-Hickey, E., Patricola, C. M., & Gallus, W. A. (2021). Anthropogenic Influences on Tornadic Storms. *Journal of Climate*, 1–57. https://doi.org/10.1175/JCLI-D-20-0901.1

Bryan, G. H., & Fritsch, J. M. (2002). A Benchmark Simulation for Moist Nonhydrostatic Numerical Models. *Monthly Weather Review*, *130*(12), 2917–2928. https://doi.org/10.1175/1520-0493(2002)130<2917:ABSFMN>2.0.CO;2

Diffenbaugh, N.S., Scherer, M., & Trapp, R. J. (2013). Robust increases in severe thunderstorm environments in response to greenhouse forcing. *Proceedings of the National Academy of Sciences of the United States of America*, *110*(41). https://doi.org/10.1073/pnas.1307758110

Elsner, J. B., Fricker, T., & Schroder, Z. (2019). Increasingly Powerful Tornadoes in the United States. *Geophysical Research Letters*, *46*(1), 392–398. https://doi.org/10.1029/2018GL080819

Frei, C., Schär, C., Lüthi, D., & Davies, H. C. (1998). Heavy precipitation processes in a warmer climate. *Geophysical Research Letters*, *25*(9), 1431–1434. https://doi.org/10.1029/98GL51099

Fricker, T., Elsner, J. B., Camp, P., & Jagger, T. H. (2014). Empirical estimates of kinetic energy from some recent U.S. tornadoes. *Geophysical Research Letters*. https://doi.org/10.1002/2014GL060441

Del Genio, A. D., Yao, M.-S., & Jonas, J. (2007). Will moist convection be stronger in a warmer climate? *Geophysical Research Letters*, *34*(16). https://doi.org/10.1029/2007GL030525

Gensini, V. A., & Brooks, H. E. (2018). Spatial trends in United States tornado frequency. *Npj Climate and Atmospheric Science 2018 1:1*, *1*(1), 1–5. https://doi.org/10.1038/s41612-018-0048-2

Gensini, V. A., Ramseyer, C., & Mote, T. L. (2014). Future convective environments using NARCCAP. *International Journal of Climatology*, *34*(5), 1699–1705. https://doi.org/10.1002/joc.3769

Hoogewind, K. A., Baldwin, M. E., & Trapp, R. J. (2017a). The Impact of Climate Change on Hazardous Convective Weather in the United States: Insight from High-Resolution Dynamical Downscaling. *Journal of Climate*, *30*, 10081–10100. https://doi.org/10.1175/JCLI-D-16-0885.1

Kimura, F., & Kitoh, A. (2007). *Downscaling by pseudo global warming method. In Final report to the ICCAP.* Kyoto, Japan.

Lepore, C., Abernathey, R., Henderson, N., Allen, J. T., & Tippett, M. K. (2021). Future Global Convective Environments in CMIP6 Models. *Earth's Future*, *n/a*(n/a), e2021EF002277. https://doi.org/https://doi.org/10.1029/2021EF002277

Markowski, P. M., Richardson, Y., Majcen, M., Marquis, J., & Wurman, J. (2011). Characteristics of the Wind Field in Three Nontornadic Low-Level Mesocyclones Observed by the Doppler On Wheels Radars. *E-Journal of Severe Storms Meteorology; Vol 6, No 3 (2011)*.

Naylor, J., & Gilmore, M. S. (2012). Convective Initiation in an Idealized Cloud Model Using an Updraft Nudging Technique. *Monthly Weather Review*, *140*(11), 3699–3705. https://doi.org/10.1175/MWR-D-12-00163.1

NCEI. (2013). NCEI Storm Events Database. Retrieved from https://www.ncdc.noaa.gov/stormevents/

NOAA. (2022). NOAA National Centers for Environmental Information (NCEI) U.S. Billion-Dollar Weather and Climate Disasters (2022). https://doi.org/10.25921/stkw-7w73

Sato, T., Kimura, F., & Kitoh, A. (2007). Projection of global warming onto regional precipitation over Mongolia using a regional climate model. *Journal of Hydrology*, *333*(1), 144–154. https://doi.org/https://doi.org/10.1016/j.jhydrol.2006.07.023

Schär, C., Frei, C., Lüthi, D., & Davies, H. C. (1996). Surrogate climate-change scenarios for regional climate models. *Geophysical Research Letters*, *23*(6), 669–672. https://doi.org/10.1029/96GL00265

Seeley, J. T., & Romps, D. M. (2015). The Effect of Global Warming on Severe Thunderstorms in the United States. *Journal of Climate*, *28*(6), 2443–2458. https://doi.org/10.1175/JCLI-D-14-00382.1

Sherburn, K. D., & Parker, M. D. (2019). The development of severe vortices within simulated high-shear, low-CAPE convection. *Monthly Weather Review*. https://doi.org/10.1175/MWR-D-18-0246.1

Skamarock, W C, Klemp, J. B., Dudhia, J., Gill, D. O., Barker, D. M., Huang, X.-Y., et al. (2008). *A description of the Advanced Research WRF version 3*. *NCAR Tech. Note TN-475+STR*.

Skamarock, William C. (2004). Evaluating Mesoscale NWP Models Using Kinetic Energy Spectra. *Monthly Weather Review*, *132*(12), 3019–3032. https://doi.org/10.1175/MWR2830.1

Strader, S. M., Ashley, W. S., Pingel, T. J., & Krmenec, A. J. (2017). Projected 21st century changes in tornado exposure, risk, and disaster potential. *Climatic Change*, *141*(2), 301–313. https://doi.org/10.1007/s10584-017-1905-4

Taylor, K. E., Stouffer, R. J., & Meehl, G. A. (2012). An Overview of CMIP5 and the Experiment Design. *Bulletin of the American Meteorological Society*, *93*(4), 485–498. https://doi.org/10.1175/BAMS-D-11-00094.1

Thompson, R. L., Smith, B. T., Grams, J. S., Dean, A. R., & Broyles, C. (2012). Convective Modes for Significant Severe Thunderstorms in the Contiguous United States. Part II:

441 Supercell and QLCS Tornado Environments. *Weather and Forecasting*, *27*(5), 1136–1154.
442 https://doi.org/10.1175/WAF-D-11-00116.1
443 Toth, M., Trapp, R. J., Wurman, J., & Kosiba, K. A. (2012). Comparison of Mobile-Radar
444 Measurements of Tornado Intensity with Corresponding WSR-88D Measurements. *Weather*
445 *and Forecasting*, *28*(2), 418–426. https://doi.org/10.1175/WAF-D-12-00019.1
446 Trapp, R.J., Woods, M. J., Lasher-Trapp, S. G., & Grover, M. A. (2021). Alternative
447 Implementations of the "Pseudo-Global-Warming" Methodology for Event-Based
448 Simulations. *Journal of Geophysical Research: Atmospheres*, *126*(24).
449 https://doi.org/10.1029/2021JD035017
450 Trapp, Robert J. (2013). *Mesoscale-Convective Processes in the Atmosphere*. Cambridge
451 University Press.
452 Trapp, Robert J, Diffenbaugh, N. S., Brooks, H. E., Baldwin, M. E., Robinson, E. D., & Pal, J. S.
453 (2007). Changes in severe thunderstorm environment frequency during the 21st century
454 caused by anthropogenically enhanced global radiative forcing. *Proceedings of the National*
455 *Academy of Sciences* , *104*(50), 19719–19723. https://doi.org/10.1073/pnas.0705494104
456 Trapp, Robert J., Diffenbaugh, N. S., & Gluhovsky, A. (2009). Transient response of severe
457 thunderstorm forcing to elevated greenhouse gas concentrations. *Geophysical Research*
458 *Letters*, *36*(1), L01703. https://doi.org/10.1029/2008GL036203
459 Trapp, Robert J, Woods, M. J., Lasher-Trapp, S. G., & Grover, M. A. (2021). Alternative
460 implementations of the "pseudo-global-warming" methodology for event-based simulations.
461 *Journal of Geophysical Research: Atmospheres*, e2021JD035017.
462 https://doi.org/https://doi.org/10.1029/2021JD035017

463 Woods, M. J. (2021). *Understanding extreme tornado events under future climate change*
464 *through the pseudo-global warming methodology*. University of Illinois at Urbana-
465 Champaign.

466

The impact of human-induced climate change on potential tornado intensity as revealed through multi-scale modeling

Matthew J. Woods[1]†, Robert J. Trapp[2], and Holly M. Mallinson[3]

[1]Department of Atmospheric Sciences, University of Illinois.

[2]Department of Atmospheric Sciences, University of Illinois.

[3]Department of Atmospheric Sciences, University of Illinois.

Corresponding author: Robert J. Trapp (jtrapp@illinois.edu)

†Current affiliation: National Weather Service, Las Vegas, NV.

Key Points:

- The effects of climate change on tornado intensity have been unclear.
- A novel, multi-modeling approach is used to address such effects.
- The intensity of cool-season tornadoes would appear to be most susceptible.

Abstract

A novel, multi-scale climate modeling approach is used to provide evidence of potential increases in tornado intensity due to anthropogenic climate change. Historical warm- and cool-season (WARM and COOL) tornado events are virtually placed in a globally warmed future via the "pseudo-global warming" method. As hypothesized based on meteorological arguments, the tornadic-storm and associated vortex of the COOL event experiences consistent and robust increases in intensity, size, and duration in an ensemble of imposed climate-change experiments. The tornadic-storm and associated vortex of the WARM event experiences increases in intensity in some of the experiments, but the response is neither consistent nor robust, and is overall weaker than in the COOL event. An examination of environmental parameters provides further support of the disproportionately stronger response in the cool-season event. These results have implications on future tornadoes forming outside of climatologically favored seasons.

1 Introduction

Hazardous convective weather (HCW) in the form of damaging winds, hail, and tornadoes poses a serious threat to life and property in the United States. From 2012 to 2022, 95 HCW events produced over $1 billion (inflation-adjusted) in damages (NOAA, 2022). The frequency of these events has increased markedly since the start of the 21st century, owing in part to increased exposure and population density (Strader et al., 2017), but also potentially to anthropogenic climate change (ACC).

HCW depends on the 3D characteristics of environmental temperature, humidity, and wind, which are projected to change under ACC. For example, warming and humidification of lower-tropospheric air yields increases in convective available potential energy (CAPE), which leads to increases in the potential intensity of convective-storm updrafts. Conversely, relatively more warming at high latitudes weakens the meridional temperature gradient and thus the vertical shear of the horizontal wind (hereinafter, VWS); this suggests a reduction in the tendency for convective updrafts to develop significant, long-lived rotational cores. General circulation model (GCM) and regional climate model (RCM) simulations project decreases in VWS that are disproportionately smaller than increases in CAPE, indicating an increase in frequency and/or

intensity of future HCW events under ACC in the United States (e.g., Del Genio et al., 2007; Trapp et al., 2007; Trapp et al., 2009; Gensini et al., 2014; Diffenbaugh et al., 2013; Seeley & Romps, 2015; Hoogewind et al., 2017). Of relevance herein is the seasonal non-uniformity to this increase: Boreal winter tends to exhibit the largest relative increase in the CAPE–VWS covariate (Diffenbaugh et al., 2013). This is consistent with historical trends of environmental parameters computed using reanalysis data (Gensini & Brooks, 2018).

Precisely how these conclusions relate to *tornado intensity*, and thus address the very basic question of whether tornadoes will tend to be more intense under ACC, is unclear. Although trends in increasingly powerful tornadoes have been revealed in historical tornado damage data in the U.S. (Elsner et al., 2019), these have not yet been physically linked to ACC. This is partly because relationships between observed tornado intensity and environmental parameters such as CAPE and VWS are ambiguous. For example, although nonzero CAPE is considered a necessary condition for, and thus critically relevant to tornadic-storm formation, CAPE alone does not correlate well with observed tornado intensity (Thompson et al., 2012). As supported by our analyses in section 3.3, a possible link could be made using multivariate environmental parameters such as the significant tornado parameter (STP), which appears to better discriminate environments of significant tornadoes from those of nonsignificant tornadoes (Thompson et al., 2012), although still not perfectly. However, an environment-only argument has a critical limitation, namely, that realization of a significant tornado is conditional on tornadic-storm initiation, which STP does not unambiguously predict. Indeed, the mean frequency of storms that initiate given a supportive environment is non-uniform in time and space, and even appears to change under ACC (Hoogewind et al., 2017).

Explicit climate modeling of tornadoes is an alternative to the use of environmental parameters and removes the storm-initiation limitation. Although such an approach has been computationally prohibitive because of the small-scale of tornadoes (~100 m to 1 km), multi-scale modeling now offers a tractable solution. Herein we employ the pseudo global warming (PGW) methodology (Schär et al., 1996; Frei et al., 1998; Kimura & Kitoh, 2007; Sato et al., 2007) using a novel, multi-scale, multi-model approach. Briefly, PGW involves a comparison of simulations of events under their true 4D environment (the control; CTRL) with those under a 4D environment modified by a climate-change perturbation representative of *mean atmospheric conditions* over future and historical time slices. Thus, the PGW method allows for an isolation of the response of an event to an imposed ACC. Because *event-level* PGW applications (see Trapp et al., 2021) involve relatively short time integrations, they also allow for the use of higher resolution and multiple realizations.

Two archetypal yet regionally and seasonally contrasting events are considered. The first is the 10 February 2013 (hereinafter, COOL) event that includes the EF-4 tornado in Hattiesburg, Mississippi, and the second is the 20 May 2013 (hereinafter, WARM) event that includes the EF-5 tornado in Moore, Oklahoma. Together, these tornadoes were responsible for 24 fatalities, more than 300 injuries, and approximately $2 billion in damage (NOAA, 2013). Our working hypothesis is that the WARM event will exhibit relatively less intensity changes under PGW than the COOL event.

Analyses of these event simulations provide the initial means to address this hypothesis. However, the spatio-temporal representations of the tornadic storms, and even the total numbers of storms, are different between the PGW and CTRL simulations (see Fig. 1). This implied lack of a clear CTRL–to–PGW comparison of *specific* tornadic storms means that a quantitative

evaluation of the climate change effect on the intensity of *specific* tornadoes is tenuous. Accordingly, we introduce an additional step wherein an idealized numerical model is integrated using initial and boundary conditions (ic/bc) drawn from the regional-model simulations. The relatively reduced complexity and higher spatial resolutions afforded by this idealized-modeling implementation of the PGW methodology helps further isolate the climate change response on a single storm, and allows for explicit diagnoses of tornado intensity.

2 Materials and Methods

2.1 PGW approach

The PGW climate modeling approach involves a simulation of some event under its actual, present-day forcing, and then simulations of the event under a modification of this forcing. The modification comes from the addition of a climate-change delta, which herein is the difference between mean conditions over future and historical time slices during a relevant month. Separate sets of deltas are constructed using historical and Representative Concentration Pathway 8.5 simulations from each of five GCMs (GFDL-CM3, MIROC5, NCAR-CCSM4, IPSL-CM5A-LR, and NorESM-1M). The GCM data originate from the Coupled Model Intercomparison Project phase 5 (Taylor et al., 2012), and provide a range of convective-storm environments over historical and future time periods (Diffenbaugh et al., 2013; Seeley & Romps, 2015).

Three different formulations of the climate-change deltas (see Trapp et al. 2021), computed using five different GCMs, provide an ensemble of 15 simulations plus an additional composite-delta simulation to assess the PGW response of each event. Because these 16 different deltas explicitly represent a range in the climate-change signal, we argue that their use toward generation of an ensemble is more relevant than other approaches. Specifically, and importantly, we are

interested in the model response to the imposed climate change and associated ic/bc rather than in the model response to variations in parameterization schemes, etc.

2.2 Regional model configuration

The CTRL and PGW simulations of the WARM and COOL events are performed using version 4.0 of the Weather Research and Forecasting model (WRF) (Skamarock et al., 2008). The parent computational domains have horizontal grid spacings of 3 km. Subdomains of 1-km grid spacing are nested within the parent domains over central Oklahoma and central Mississippi, respectively (Fig. S1). The results reported in section 3.1 are based on analyses over the nested domains.

The simulations are initialized at 12 UTC for both events. This allows for more than six hours of "spin-up" time prior to the observed EF-5 Moore and EF-4 Hattiesburg tornadoes, which is typical for weather-event simulations with WRF (Skamarock, 2004). Initial and boundary conditions are derived from the North American Mesoscale Forecast System analysis. Additional details regarding WRF model configuration can be found in Trapp et al. (2021). Decisions on the configuration and on the ultimate veracity of the CTRL simulations were established by comparing model output from configuration-sensitivity experiments to observed radar characteristics and tornado reports, as described in Woods (2021).

Upon adapting the approach of Sherburn & Parker (2019), local tornado occurrence and potential intensity are diagnosed using the Okubo-Weiss (OW) parameter. OW is computed at 80 m AGL as the difference between vertical vorticity squared and deformation squared (e.g., Markowski et al., 2011); the choice of 80 m is based on its use in operational applications. At the 1-km gridpoint spacings of the WRF simulations, tornadoes are still unresolved, so OW is used

as a proxy: An OW value locally exceeding 3.5×10^{-5} s^{-2}, which is the 90th percentile of all gridpoint values with positive OW in the CTRL simulation, serves as a tornado proxy occurrence. An OW value exceeding 6×10^{-5} s^{-2}, which is the 95th percentile, serves as a significant tornado proxy occurrence. Coexistence of local updraft velocities exceeding 5 m s^{-1} is also required. Differentiating tornado intensity based on OW and thus tornadic-circulation strength follows from Doppler radar-based studies of Toth et al. (2012) and others. Owing in part to the discreteness of the OW calculations, there is no expectation of a one-to-one correspondence between the numbers of tornadoes and tornado proxies. Rather, the proxy occurrences should be viewed in a relative sense, which is how the results are presented in section 3.1.

2.3 Idealized model configuration

The idealized simulations are performed using Cloud Model 1 (CM1) (Bryan & Fritsch, 2002). Grid stretching is employed such that the horizontal grid spacing is 64 m over the inner 80 x 80 km of the 180 x 180 x 18.5 km model domain, and then increased to 2.5 km at the domain edges. Vertical grid spacing is stretched from 20 m in the lowest 300 m to 250 m in the upper 6000 m, with 125 m grid spacing in between. Additional details regarding the CM1 model configuration can be found in Woods (2021). Note that the actual tornadoes that occurred on 20 May 2013 and 10 February 2013 had damage widths of 1600 m and 1200 m, respectively. Even if the core diameters of maximum winds of these tornadoes were 50% of these widths, the cores would still be represented by ~10 grid points. So, although our simulations do not have grid spacings appropriate to resolve fine-scale structures of the tornadoes, the simulations are

certainly sufficient to represent core widths and windspeeds, which is one goal of these simulations.

The initial and boundary conditions are drawn from the WRF output of the CTRL and PGW simulations. Specifically, 60 x 60 km horizontal averages centered about the WRF grid point nearest to Moore, Oklahoma and Hattiesburg, Mississippi are used to obtain vertical profiles at 20 UTC 20 May 2013 and 23 UTC 10 February, respectively, which represent well the pre-tornadic conditions during these two events. A single deep convective storm is initiated within these environments via updraft nudging (Naylor & Gilmore, 2012) that persisted for 20 minutes. Our analysis of the subsequent tornadic circulations began at 30 min, i.e., 10 min after the cessation of the nudging.

Tornadic-like vortices (TLVs) are identified by examining near-surface fields of windspeed, vertical vorticity, and OW parameter. Following Sherburn & Parker (2019), TLV identification required vertical vorticity, windspeed, and OW to exceed 0.1 s^{-1}, 30 m s^{-1}, and 0.03 s^{-2}, respectively, and be collocated with low-level updraft speeds exceeding 5 m s^{-1}. Upon locating the strongest TLV, maximum and minimum of *x*-direction and *y*-direction wind components are found within 500 m of the vortex center. The locations of these maxima and minima are used to determine an average radius (r) of maximum winds (V).

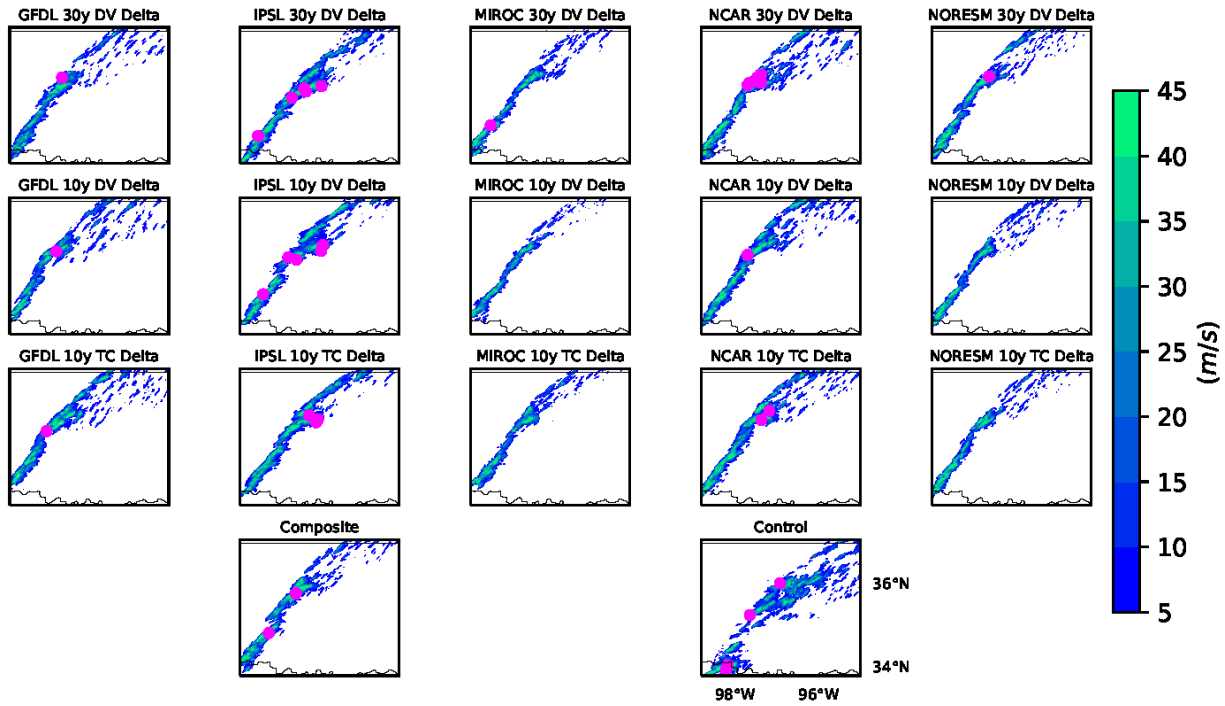

177

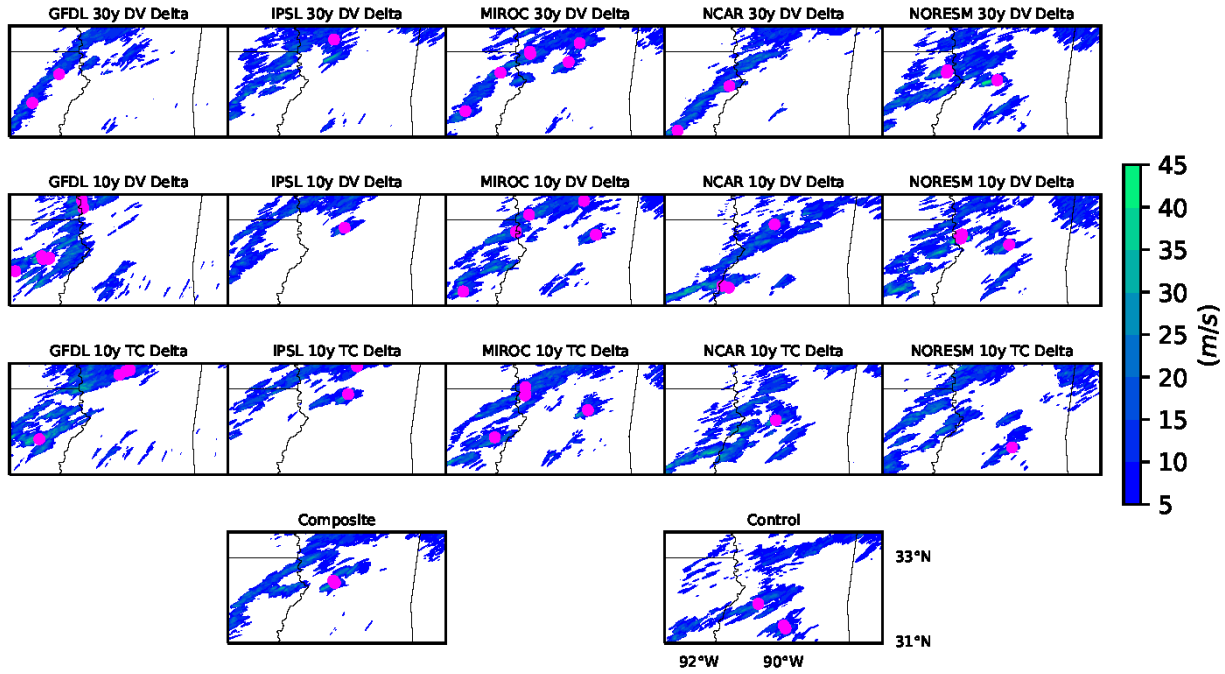

178

179 **Figure 1.** Locations of model-diagnosed tornadic circulations (magenta dots) and column-
180 maximum updraft speeds (m s^{-1}) for the regional-modeling simulations of the WARM event at
181 2100 UTC (upper panels), and COOL event at 2230 UTC (lower panels). In addition to the
182 CTRL simulation, the subpanels indicate an individual experiment composing the ensemble.
183

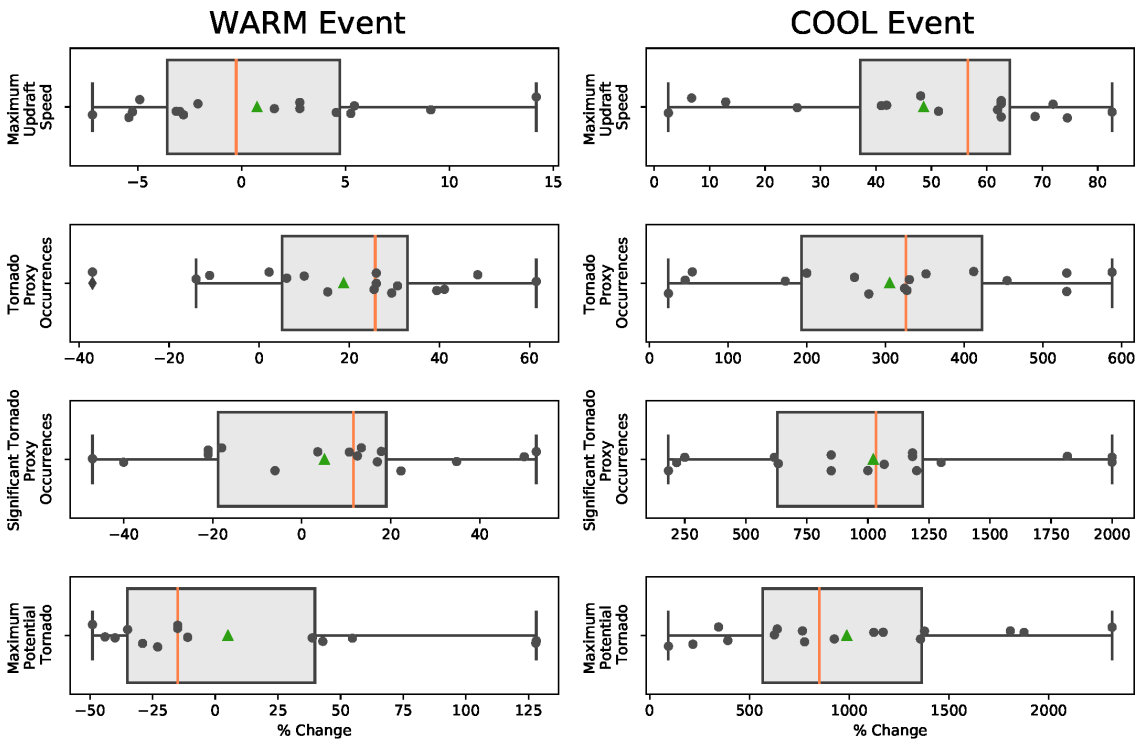

Figure 2. Box-and-whisker plots of tornadic-storm intensity metrics, as evaluated from the regional modeling simulations of the WARM event (left) and COOL event (right). Values of these metrics are given as percentage changes in the PGW simulations relative to the control (CTRL) simulation. The median is the orange line, mean is the green triangle, and individual data points are the black circles.

3 Results

3.1 Regional-modeling perspective

An ensemble of 16 simulations is used to assess the PGW response of each event. The ensemble members are meant to represent a range of possible future realizations of the event. Herein, if 75% of the ensemble members exhibit the same sign in the percentage change (PGW relative to CTRL) in a given metric, we consider the PGW response for that metric to be *consistent*. If we equate the signal in the metric to the mean value across the ensemble, and the

noise to the standard deviation, the response in this metric is considered to be *robust* (*highly robust*) if the PGW signal-to-noise ratio in a given metric exceeds one (two) (e.g., Diffenbaugh et al., 2013).

We begin with two metrics that provide information on overall storm intensity. The first is the cumulative gridpoint exceedance of 55 dBZ simulated radar reflectivity (Fig. S2). This metric quantifies the total area of intense convective storms over a given simulation. A consistent, robust response is shown in this metric, as represented by an average percentage increase of +110% (PGW exceedances relative to those in the CTRL) (Fig. 2a). Thus, the PGW-modified conditions resulted in relatively more extensive and intense convective storms in association with the WARM event.

Cumulative gridpoint exceedances of simulated updraft speed confirm this increase in the extent of intense convective storms under PGW (Fig. S3); this consistent, robust response is represented by an average percentage increase of +40%. The *peak* updraft speeds are comparatively stronger in only half of the PGW simulations, with an average percentage increase of +1% (Fig. 2). These results indicate that intense convective updrafts in a future realization of the WARM event would be more numerous or larger, but not always stronger.

In terms of the occurrences of our tornado proxy, the PGW response is inconsistent albeit robust, with a mean percentage *decrease* of -7% (Fig. 2). For occurrences of our significant tornado proxy, the mean response is inconsistent but highly robust, with a mean percentage decrease of -19% (Fig. 2). Finally, when we evaluate the peak OW per PGW simulation, which provides some information about the potential tornado intensity, we find this response to be consistently negative but not robust, with an average percentage difference (PGW values relative

to those in the CTRL) of -11% (Fig. 2). Thus, the regional modeling suggests relatively fewer and weaker tornadoes in the WARM event under PGW, albeit with uncertainty (see also Fig. 1).

Like the WARM event, the COOL event under PGW also tends to be characterized by more intense convective storms. Specifically, cumulative gridpoint exceedances of simulated reflectivity of 55 dBZ are greater in all but one of the PGW simulations, thus contributing to an average percentage increase of +125%, and a consistent and robust response in this metric (Fig. S2). The other metric for overall storm intensity, cumulative gridpoint exceedances of updraft speed of 25 m s^{-1}, is consistent but not robust; notably, the average percentage increase in such strong updraft occurrence in the COOL event is +712%, as compared to the +40% increase associated with the WARM event (see Fig. S3). *All* PGW simulations had peak updraft speeds exceeding the 31 m s^{-1} peak of the CTRL (Fig. 2), thus implying a consistent and robust response. Moreover, half of the PGW simulations had peak updrafts exceeding 50 m s^{-1}, which historically are speeds more readily supportive in warm-season, Great Plains environments than in cool-season, southeast U.S. environments. These results indicate that intense convective updrafts in a future realization of the COOL event would be more numerous *and* stronger.

Occurrences of the tornado proxy are substantially greater under PGW in many of the simulations, leading to an average percentage increase relative to CTRL of +163% (Fig. 2). Occurrences of the significant tornado proxy are also substantially greater, with an average percentage increase of +642%, in this consistent and robust response (Fig. 2). Finally, a consistent and robust response is indicated in the peak OW per PGW simulation, and thus potential tornado intensity, with an average percentage increase of +756% (Fig. 2).

Collectively, these results suggest that tornadic circulations in a future realization of the COOL event would be more numerous, stronger, and perhaps longer-lived. In agreement with

our hypothesis, the magnitude of the response of this archetypal cool-season event to PGW is much larger than that of the archetypal warm-season event; this finding is also in agreement with Bercos-Hickey et al. (2021). There is still, however, ambiguity in precisely how the analyzed response relates to tornado intensity, given both the model grid resolution and the nature of the tornado proxy. Thus, we now use the TLV–resolving idealized PGW simulations to compute explicit measures of tornado intensity, and thus help clarify the regional-model results.

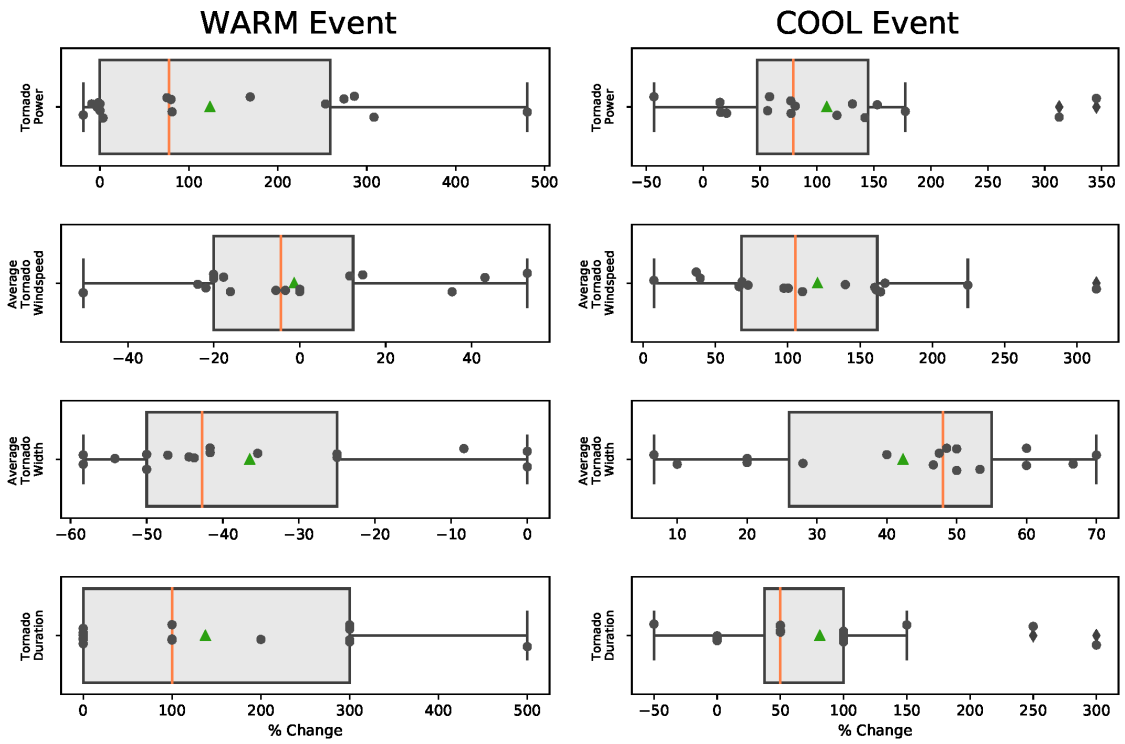

Figure 3. As in Figure 2, except for tornado intensity metrics (see text).

3.2 Idealized modeling perspective

The idealized PGW simulations have steady, horizontally homogeneous initial and boundary conditions that were drawn from the regional-model simulations of the WARM and COOL events (Figs. S4-S5). The much finer grid spacings (64 m) allow for explicit

quantifications of TLVs that form within the simulated storms. For this we use *tornado power*, which accounts for the tornadic wind speed as well as the width and length of the tornado track. As adapted from Fricker et al. (2014), instantaneous tornado power can be calculated as

$$P = \pi r^2 \rho V^3 \qquad (1)$$

where r represents the average radius of maximum winds, ρ is the air density (assumed to be 1 kg m^{-3}), and V is the average maximum surface wind speed at radius r. Total tornado power here is the summation of $\log(P)$ over the lifetime of the tornado-like vortex,

$$P_t = \sum \log(P) \qquad (2)$$

In simulations of the WARM event, the PGW response in total power is neither consistent nor robust. However, the 16-member ensemble contributed to an average percentage increase in P_t of +124% (Fig. 3). This average percentage increase is due to a few experiments with relatively stronger vortex windspeeds; none of the experiments exhibited wider vortices (Fig. 3). Thus, as in the coarser-resolution regional modeling simulations, there are indications of intensity increases in this violent, Great Plains, warm-season tornado given an imposed climate change.

For the COOL event, the PGW response in total power is both consistent and robust, with an average percentage increase of +109% (Fig. 3). The increases in P_t are driven by consistent and robust increases in tornadic-vortex strength and width (Fig. 3). The relatively longer duration of the tornadic vortices (+81%) also contribute to the larger P_t under PGW. These high-resolution simulations are in agreement with the regional modeling simulations, and clearly demonstrate an increased intensity and duration for this archetypal cool-season tornado given an imposed climate change. The collective simulations also confirm our hypothesis regarding a relatively larger response of this cool-season event.

Table 1. Mean values, and percentage changes relative to the CTRL experiment, of environmental parameters computed from the initial/boundary conditions of the idealized-modeling PGW experiments.

Event	CAPE (J/kg)		CIN (J/kg)		LCL (m)		SRH3 (m2/s2)		SRH1 (m2/s2)		S06 (m/s)		STP	
WARM	4484	+56	0	+100	1774	+23	86	-58	34	-53	24	-14	0.2	-72
COOL	1037	+162	-24	-61	243	+33	427	-21	327	-23	36	-4	2.2	+100

CIN is convective inhibition; LCL is lifting condensation level; SRH3 is storm-relative environmental helicity, evaluated over the 0-3 km layer; SRH1 is storm-relative environmental helicity, evaluated over the 0-1 km layer; S06 is the bulk wind shear, evaluated over the 0-6 km layer.

We can use the ic/bc of the idealized experiments to explore the meteorological arguments on which this hypothesis is based. The mean, PGW-enhanced CAPE of 4484 J kg^{-1} and 1037 J kg^{-1} for the WARM and COOL events, respectively, represent consistent and robust increases of +56% and +162% relative to the corresponding CTRL environments (Table 1). The mean, PGW-diminished VWS of 24 m s^{-1} and 36 m s^{-1} for the WARM and COOL events, respectively, represent consistent and robust decreases of -14% and -4% relative to the corresponding CTRL environments (Table 1); disproportionate decreases of storm-relative helicity, another measure of VWS, are also revealed for the WARM versus COOL events (-53% and -23%, respectively; Table 1). When these and other environmental parameters are combined through the multivariate parameter STP, the environment of the WARM event is found to be relatively *less* supportive of a significant tornado under PGW (mean percentage decrease of -73%), while the environment of the COOL event is relatively *more* supportive under PGW (mean percentage increase of +100%) (Table 1).

3.3 Generality of the conclusions

306 Although the intensity changes described herein apply to the specific WARM and COOL
307 events simulated, all potential tornadic-storm events realized during the warm- and cool-season
308 months of consideration would be subject to the same range of climate-change perturbations. To
309 help quantify how these perturbations alone might contribute to environments of significant
310 tornadoes, STP is calculated at all points within the regional-model domain for the CTRL and
311 PGW simulations of both events (Fig. S7). Upon spatially averaging the PGW – CTRL
312 differences, we find that the ensemble mean STP perturbation is -0.30 for the month of May, and
313 +0.70 for the month of February. The implication is that ACC would contribute, *on average*, to
314 environments that are relatively *less* supportive of a significant tornado during May across the
315 central Great Plains U.S., and relatively *more* supportive of a significant tornado during February
316 across the southeast U.S. Such environmental changes have been noted in studies by Gensini &
317 Brooks (2018), Bercos-Hickey et al. (2021), and Lepore et al. (2021).

318

319 **4 Summary and Conclusions**

320 Although trends in increasingly powerful tornadoes have been suggested in historical
321 data on tornado damage (Elsner et al., 2019), our study is the first to provide evidence of
322 potential increases in future tornado intensity due to ACC.

323 This statement applies explicitly to two contemporary, archetypal, warm- and cool-season
324 tornado events that were virtually placed in a globally warmed future via the PGW method.
325 Specifically, the consistent and robust increases in intensity, size, and duration of the tornadic-
326 storm and associated vortex of the COOL event can be attributed directly to ACC. The lack of a
327 consistent and robust increase in the intensity of the tornadic-storm and associated vortex of the

WARM event can likewise be attributed directly to ACC. Consideration of other data lends support to such a disproportionate response based on season of the year.

The preceding statement should not be interpreted to mean that *all* tornadoes will be stronger in the future. The atmospheric heterogeneity arising from naturally variable large-scale atmospheric circulations, high-frequency weather systems, convective storms and their residual effects, and land-surface variations (e.g., see Trapp, 2013) will continue to create diverse environmental conditions both supportive and non-supportive of thunderstorm formation. Significant tornadogenesis within such thunderstorms will also continue to require a delicate balance between VWS and CAPE, among other environmental parameters. Yet because cool-season environments in the current climate tend to be characterized by very large VWS and small CAPE, future increases in CAPE (decreases in VWS) due to ACC appear to be relatively more conductive to (less impactful on) this balance and thus on cool-season tornado potential.

These findings have implications on the possible impacts of future tornadoes forming outside of climatologically favored seasons, in the United States and elsewhere around the world. Indeed, situational awareness of tornado risk tends to be reduced during seasons such as boreal winter, which offers one explanation for high fatalities from tornadic events during these times (e.g., Ashley, 2007). It follows that more intense future tornadoes would have the potential to result in more fatalities and damage.

Acknowledgments

This research was supported by the National Science Foundation, award AGS 1923042. The WRF simulations were conducted on the NCAR Cheyenne Computing Facility. The CM1 simulations were conducted on the Blue Waters Petascale Computing Facility. We thank Dr.

George Bryan for making available and otherwise supporting the CM1 model. We acknowledge the World Climate Research Programme's Working Group on Coupled Modelling, which is responsible for CMIP, and we thank the climate modeling groups indicated in section 2.1 for producing and making available their model output.

Open Research

The following GCM data sets used in this study are available through the CMIP5 repository (https://esgf-node.llnl.gov/projects/cmip5/), using these criteria: Models: GFDL-CM3, MIROC5, NCAR-CCSM4, IPSL-CM5A-LR, and NorESM-1M; Experiments: historical and RCP8.5; Ensemble: r1i1p1; Realm: atmos; and Time Frequency: 3hr or 6hr. The WRF model is available at https://www2.mmm.ucar.edu/wrf/users/, and the CM1 model is available at https://www2.mmm.ucar.edu/people/bryan/cm1/. Relevant simulation data are available through the Illinois Data Bank at https://databank.illinois.edu/datasets/IDB-4479773#.

References

Ashley, W. S. (2007). Spatial and Temporal Analysis of Tornado Fatalities in the United States: 1880–2005. *Weather and Forecasting*, *22*(6), 1214–1228. https://doi.org/10.1175/2007WAF2007004.1

Bercos-Hickey, E., Patricola, C. M., & Gallus, W. A. (2021). Anthropogenic Influences on Tornadic Storms. *Journal of Climate*, 1–57. https://doi.org/10.1175/JCLI-D-20-0901.1

Bryan, G. H., & Fritsch, J. M. (2002). A Benchmark Simulation for Moist Nonhydrostatic Numerical Models. *Monthly Weather Review*, *130*(12), 2917–2928. https://doi.org/10.1175/1520-0493(2002)130<2917:ABSFMN>2.0.CO;2

Diffenbaugh, N.S., Scherer, M., & Trapp, R. J. (2013). Robust increases in severe thunderstorm environments in response to greenhouse forcing. *Proceedings of the National Academy of Sciences of the United States of America*, *110*(41). https://doi.org/10.1073/pnas.1307758110

Elsner, J. B., Fricker, T., & Schroder, Z. (2019). Increasingly Powerful Tornadoes in the United States. *Geophysical Research Letters*, *46*(1), 392–398. https://doi.org/10.1029/2018GL080819

Frei, C., Schär, C., Lüthi, D., & Davies, H. C. (1998). Heavy precipitation processes in a warmer climate. *Geophysical Research Letters*, *25*(9), 1431–1434. https://doi.org/10.1029/98GL51099

Fricker, T., Elsner, J. B., Camp, P., & Jagger, T. H. (2014). Empirical estimates of kinetic energy from some recent U.S. tornadoes. *Geophysical Research Letters*. https://doi.org/10.1002/2014GL060441

Del Genio, A. D., Yao, M.-S., & Jonas, J. (2007). Will moist convection be stronger in a warmer climate? *Geophysical Research Letters*, *34*(16). https://doi.org/10.1029/2007GL030525

Gensini, V. A., & Brooks, H. E. (2018). Spatial trends in United States tornado frequency. *Npj Climate and Atmospheric Science 2018 1:1*, *1*(1), 1–5. https://doi.org/10.1038/s41612-018-0048-2

Gensini, V. A., Ramseyer, C., & Mote, T. L. (2014). Future convective environments using NARCCAP. *International Journal of Climatology*, *34*(5), 1699–1705. https://doi.org/10.1002/joc.3769

Hoogewind, K. A., Baldwin, M. E., & Trapp, R. J. (2017a). The Impact of Climate Change on Hazardous Convective Weather in the United States: Insight from High-Resolution Dynamical Downscaling. *Journal of Climate*, *30*, 10081–10100. https://doi.org/10.1175/JCLI-D-16-0885.1

Kimura, F., & Kitoh, A. (2007). *Downscaling by pseudo global warming method. In Final report to the ICCAP.* Kyoto, Japan.

Lepore, C., Abernathey, R., Henderson, N., Allen, J. T., & Tippett, M. K. (2021). Future Global Convective Environments in CMIP6 Models. *Earth's Future*, *n/a*(n/a), e2021EF002277. https://doi.org/https://doi.org/10.1029/2021EF002277

Markowski, P. M., Richardson, Y., Majcen, M., Marquis, J., & Wurman, J. (2011). Characteristics of the Wind Field in Three Nontornadic Low-Level Mesocyclones Observed by the Doppler On Wheels Radars. *E-Journal of Severe Storms Meteorology; Vol 6, No 3 (2011)*.

Naylor, J., & Gilmore, M. S. (2012). Convective Initiation in an Idealized Cloud Model Using an Updraft Nudging Technique. *Monthly Weather Review*, *140*(11), 3699–3705. https://doi.org/10.1175/MWR-D-12-00163.1

NCEI. (2013). NCEI Storm Events Database. Retrieved from https://www.ncdc.noaa.gov/stormevents/

NOAA. (2022). NOAA National Centers for Environmental Information (NCEI) U.S. Billion-Dollar Weather and Climate Disasters (2022). https://doi.org/10.25921/stkw-7w73

Sato, T., Kimura, F., & Kitoh, A. (2007). Projection of global warming onto regional precipitation over Mongolia using a regional climate model. *Journal of Hydrology*, *333*(1), 144–154. https://doi.org/https://doi.org/10.1016/j.jhydrol.2006.07.023

Schär, C., Frei, C., Lüthi, D., & Davies, H. C. (1996). Surrogate climate-change scenarios for regional climate models. *Geophysical Research Letters*, *23*(6), 669–672. https://doi.org/10.1029/96GL00265

Seeley, J. T., & Romps, D. M. (2015). The Effect of Global Warming on Severe Thunderstorms in the United States. *Journal of Climate*, *28*(6), 2443–2458. https://doi.org/10.1175/JCLI-D-14-00382.1

Sherburn, K. D., & Parker, M. D. (2019). The development of severe vortices within simulated high-shear, low-CAPE convection. *Monthly Weather Review*. https://doi.org/10.1175/MWR-D-18-0246.1

Skamarock, W C, Klemp, J. B., Dudhia, J., Gill, D. O., Barker, D. M., Huang, X.-Y., et al. (2008). *A description of the Advanced Research WRF version 3*. *NCAR Tech. Note TN-475+STR*.

Skamarock, William C. (2004). Evaluating Mesoscale NWP Models Using Kinetic Energy Spectra. *Monthly Weather Review*, *132*(12), 3019–3032. https://doi.org/10.1175/MWR2830.1

Strader, S. M., Ashley, W. S., Pingel, T. J., & Krmenec, A. J. (2017). Projected 21st century changes in tornado exposure, risk, and disaster potential. *Climatic Change*, *141*(2), 301–313. https://doi.org/10.1007/s10584-017-1905-4

Taylor, K. E., Stouffer, R. J., & Meehl, G. A. (2012). An Overview of CMIP5 and the Experiment Design. *Bulletin of the American Meteorological Society*, *93*(4), 485–498. https://doi.org/10.1175/BAMS-D-11-00094.1

Thompson, R. L., Smith, B. T., Grams, J. S., Dean, A. R., & Broyles, C. (2012). Convective Modes for Significant Severe Thunderstorms in the Contiguous United States. Part II:

441 Supercell and QLCS Tornado Environments. *Weather and Forecasting*, *27*(5), 1136–1154.
442 https://doi.org/10.1175/WAF-D-11-00116.1
443 Toth, M., Trapp, R. J., Wurman, J., & Kosiba, K. A. (2012). Comparison of Mobile-Radar
444 Measurements of Tornado Intensity with Corresponding WSR-88D Measurements. *Weather*
445 *and Forecasting*, *28*(2), 418–426. https://doi.org/10.1175/WAF-D-12-00019.1
446 Trapp, R.J., Woods, M. J., Lasher-Trapp, S. G., & Grover, M. A. (2021). Alternative
447 Implementations of the "Pseudo-Global-Warming" Methodology for Event-Based
448 Simulations. *Journal of Geophysical Research: Atmospheres*, *126*(24).
449 https://doi.org/10.1029/2021JD035017
450 Trapp, Robert J. (2013). *Mesoscale-Convective Processes in the Atmosphere*. Cambridge
451 University Press.
452 Trapp, Robert J, Diffenbaugh, N. S., Brooks, H. E., Baldwin, M. E., Robinson, E. D., & Pal, J. S.
453 (2007). Changes in severe thunderstorm environment frequency during the 21st century
454 caused by anthropogenically enhanced global radiative forcing. *Proceedings of the National*
455 *Academy of Sciences* , *104*(50), 19719–19723. https://doi.org/10.1073/pnas.0705494104
456 Trapp, Robert J., Diffenbaugh, N. S., & Gluhovsky, A. (2009). Transient response of severe
457 thunderstorm forcing to elevated greenhouse gas concentrations. *Geophysical Research*
458 *Letters*, *36*(1), L01703. https://doi.org/10.1029/2008GL036203
459 Trapp, Robert J, Woods, M. J., Lasher-Trapp, S. G., & Grover, M. A. (2021). Alternative
460 implementations of the "pseudo-global-warming" methodology for event-based simulations.
461 *Journal of Geophysical Research: Atmospheres*, e2021JD035017.
462 https://doi.org/https://doi.org/10.1029/2021JD035017

463 Woods, M. J. (2021). *Understanding extreme tornado events under future climate change*
464 *through the pseudo-global warming methodology*. University of Illinois at Urbana-
465 Champaign.

466

The impact of human-induced climate change on potential tornado intensity as revealed through multi-scale modeling

Matthew J. Woods[1]†, Robert J. Trapp[2], and Holly M. Mallinson[3]

[1]Department of Atmospheric Sciences, University of Illinois.

[2]Department of Atmospheric Sciences, University of Illinois.

[3]Department of Atmospheric Sciences, University of Illinois.

Corresponding author: Robert J. Trapp (jtrapp@illinois.edu)

†Current affiliation: National Weather Service, Las Vegas, NV.

Supplementary Material

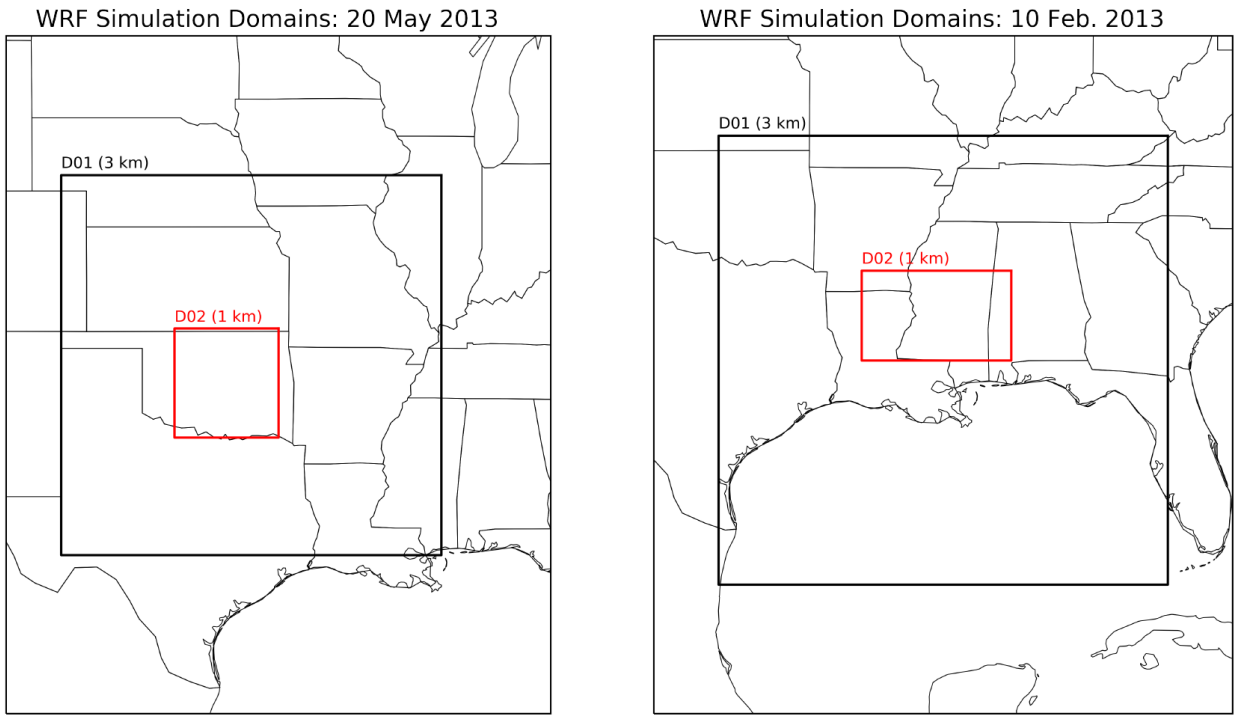

Supplemental Figure S1. Computational domains used for the regional model (WRF) simulations of the 20 May 2013 (WARM) and 10 February 2013 (COOL) events.

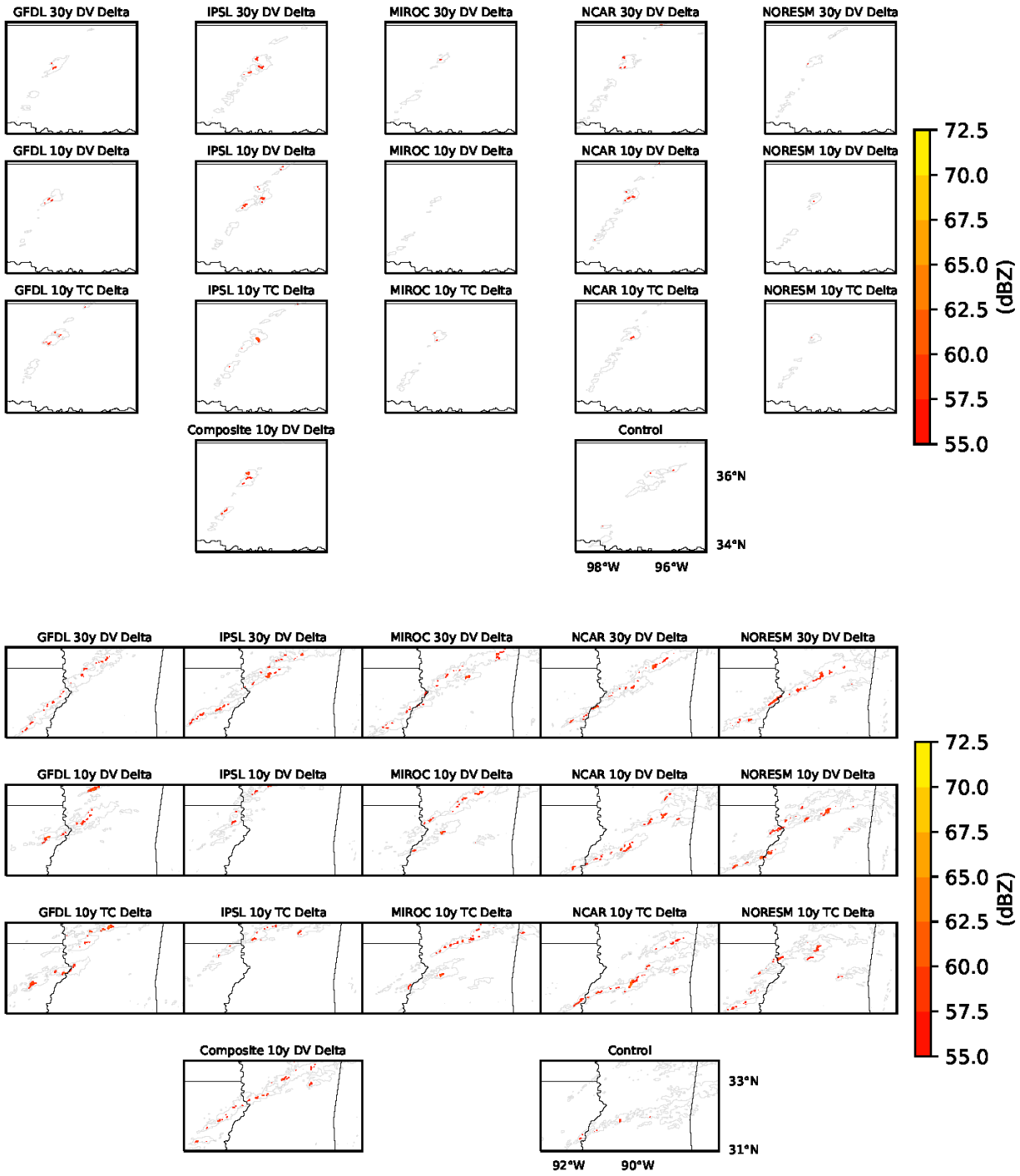

Supplemental Figure S2. Simulated radar reflectivity (dBZ) for the regional-modeling simulations of the WARM event (top panel; 2100 UTC) and COOL event (bottom panel; 0000 UTC). The color fill indicates the areas of intense convective storms over a given simulation. The gray contours are of 30 dBZ radar reflectivity, and show the outline of the convective storms. Each subpanel represents an individual experiment composing the ensemble. See section 2 for guidance on experiment nomenclature.

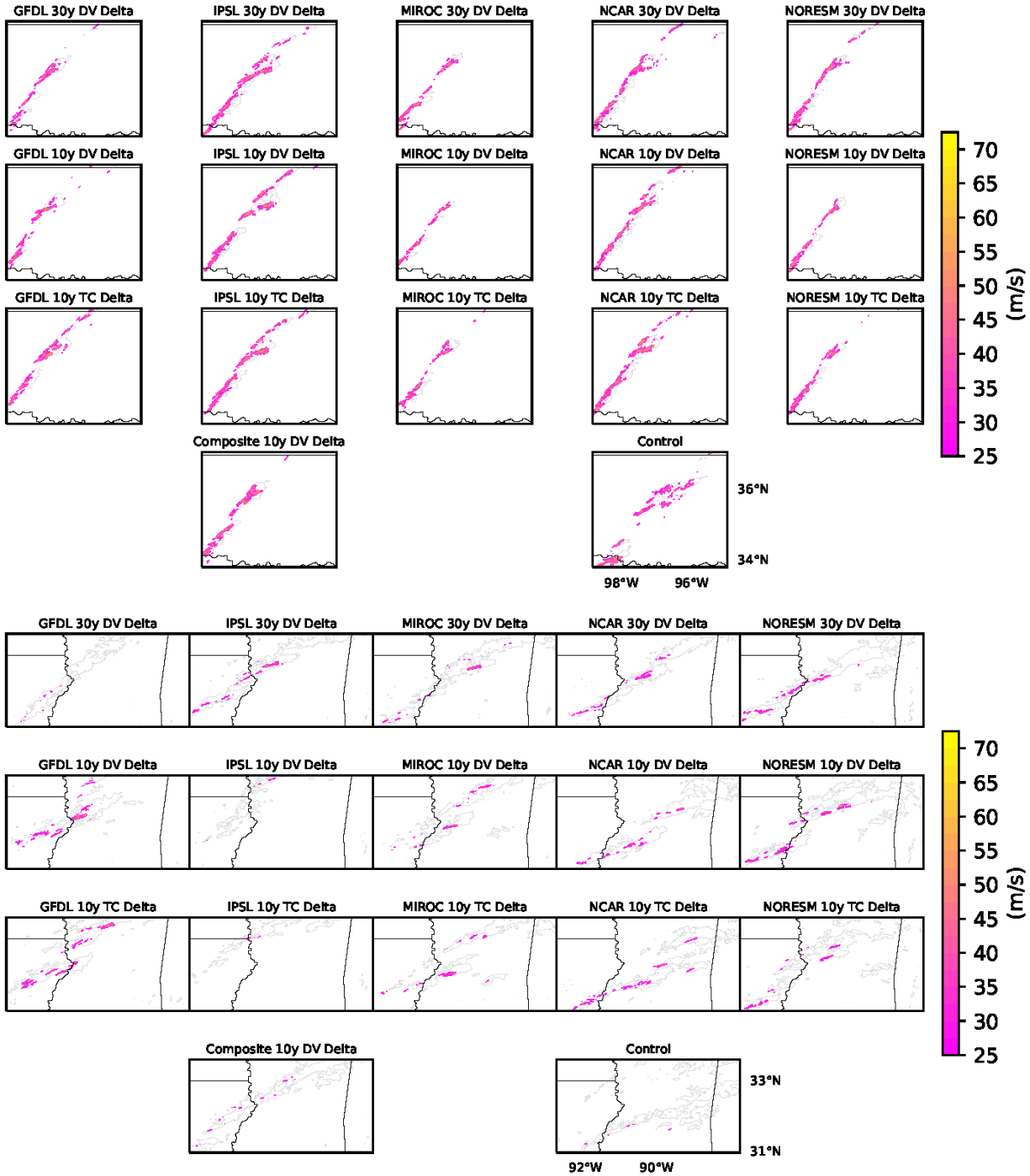

Supplemental Figure S3. Maximum vertical velocity (m/s) for the regional-modeling simulations of the WARM event (top panel; 2100 UTC) and COOL event (bottom panel; 0000 UTC). The color fill indicates the areas of intense updrafts over a given simulation. The gray contours are of 30 dBZ radar reflectivity, and show the outline of the convective storms. Each subpanel represents an individual experiment composing the ensemble. See section 2 for guidance on experiment nomenclature.

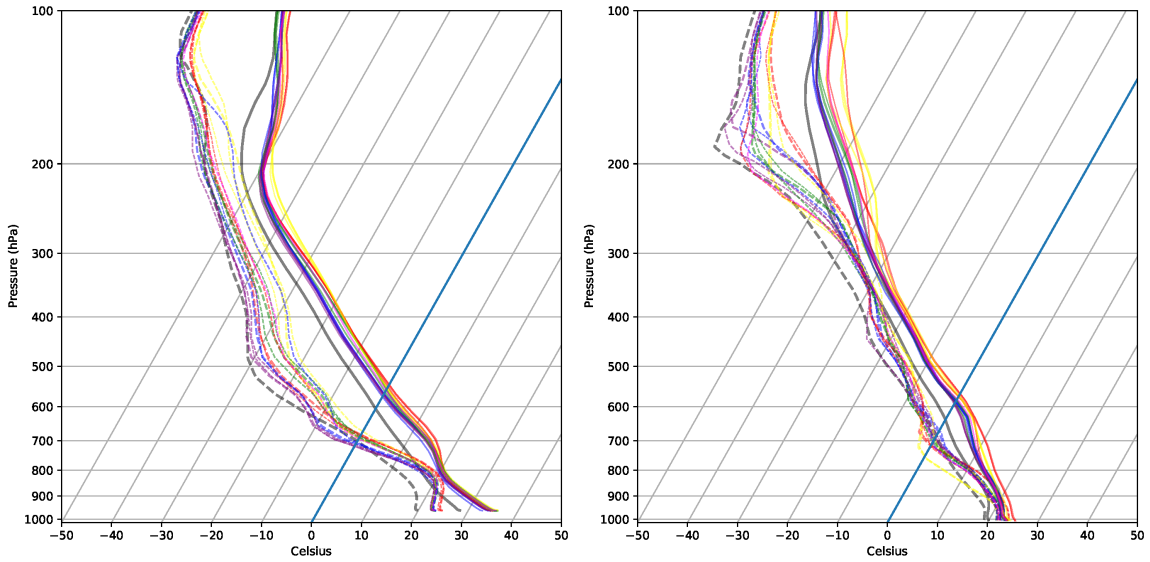

Supplemental Figure S4. Initial and boundary conditions of temperature and dewpoint (°C) for the idealized modeling simulations, for the WARM event (left panel) and COOL event (right panel), as presented on skew-T/log-p diagrams. The solid and dashed black (colored) lines are the temperature and dewpoint for the CTRL (PGW) simulations.

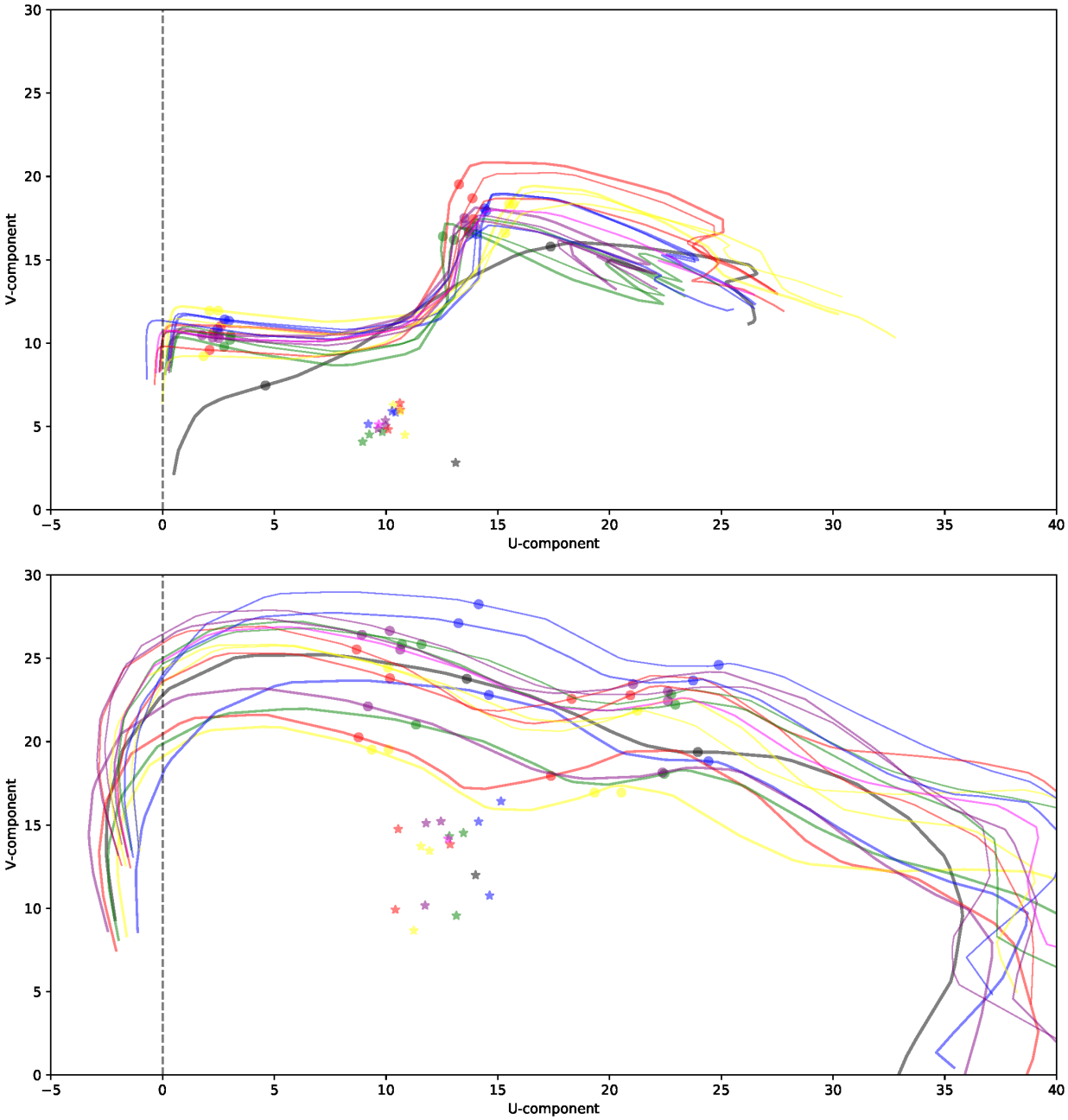

Supplemental Figure S5. Initial and boundary conditions of horizontal wind components (m/s), for the WARM event (top panel) and COOL event (bottom panel), as presented on hodograph plots. The solid (colored) lines are for the CTRL (PGW) simulations. Asterisks show estimated storm motion for a right-moving supercell, and closed circles indicate heights of 1 and 3 km.

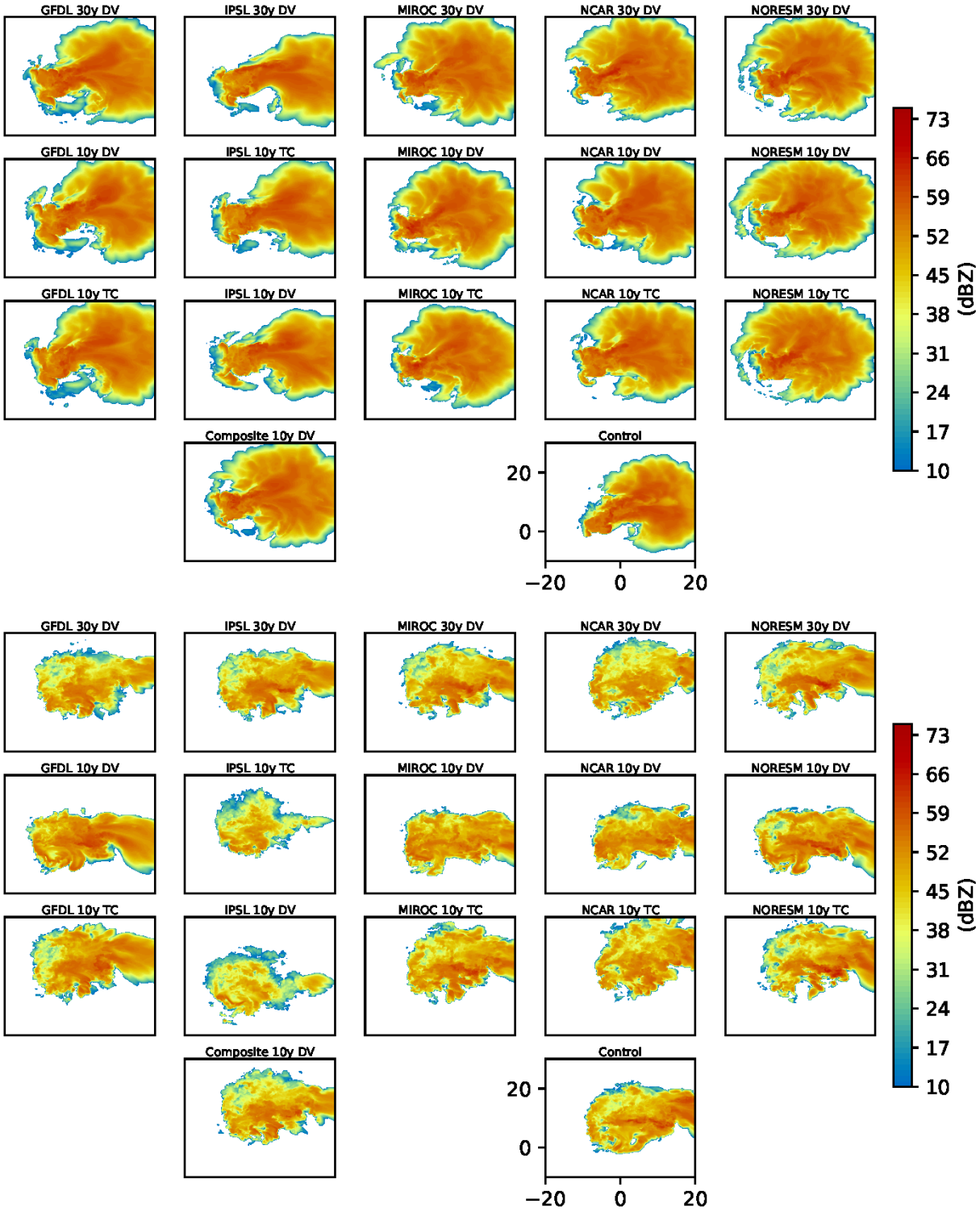

Supplemental Figure S6. Simulated radar reflectivity (dBZ) for the idealized-modeling simulations of the WARM event (top panel) and COOL event (bottom panel) at 30 min. Each subpanel represents an individual experiment composing the ensemble. See section 2 for guidance on experiment nomenclature.

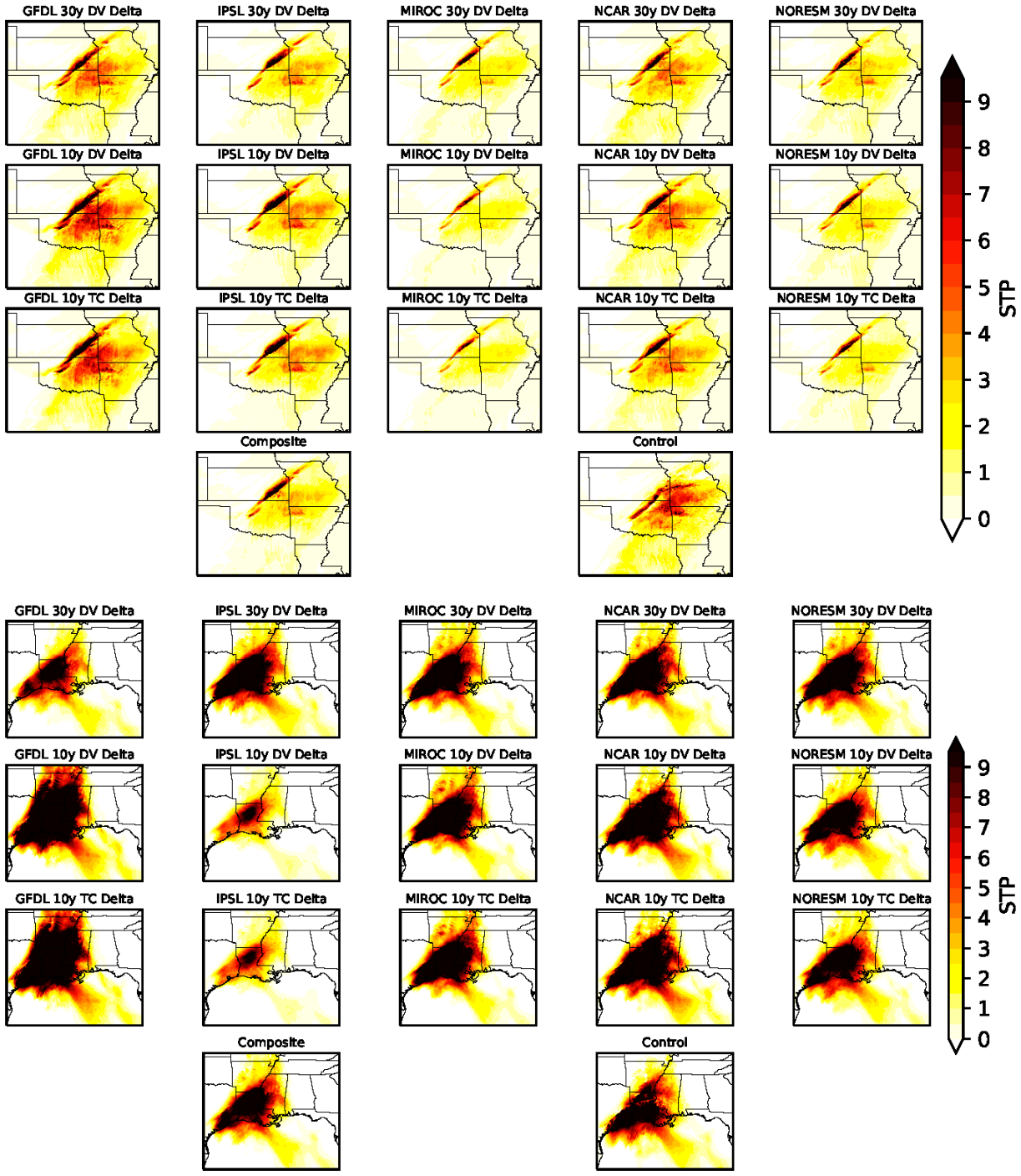

Supplemental Figure S7. Analysis of the significant tornado parameter (STP; nondimensional) over the respective simulation domains (D01; see Fig. S1) of the WARM event (top panel) and COOL event (bottom panel). The calculations were performed using model output at 1800 UTC for the WARM event, and 1500 UTC for the COOL event, which generally represent pre-convective times across the respective simulation domains. See section 2 for guidance on experiment nomenclature.